Atomization and Powder Processing of High Temperature Ferritic Stainless Steel

Iver E. Anderson[1], ***Joel R. Rieken[1,2]***, ***David J. Byrd[1]***

[1]Division of Materials Sciences and Engineering, Ames Laboratory (USDOE), Ames, IA
[2]Materials Science and Engineering Department, Iowa State University, Ames, IA

26th Annual Conference on Fossil Energy Materials

Pittsburgh, PA

April 18, 2012

Support from DOE-Fossil Energy-Advanced Research Materials Program is gratefully acknowledged through Ames Laboratory contract no. DE-AC02-07CH11358

Application Goals

➢ **Create a simplified process for production of precursor powders and oxide dispersion strengthened ferritic stainless steel alloys**

A-USC Steam Coal Fired:

- Boiler / Burner Materials
- Heat exchanger tubing
- Exhaust liner
- 760ºC at 35MPa Supercritical Steam

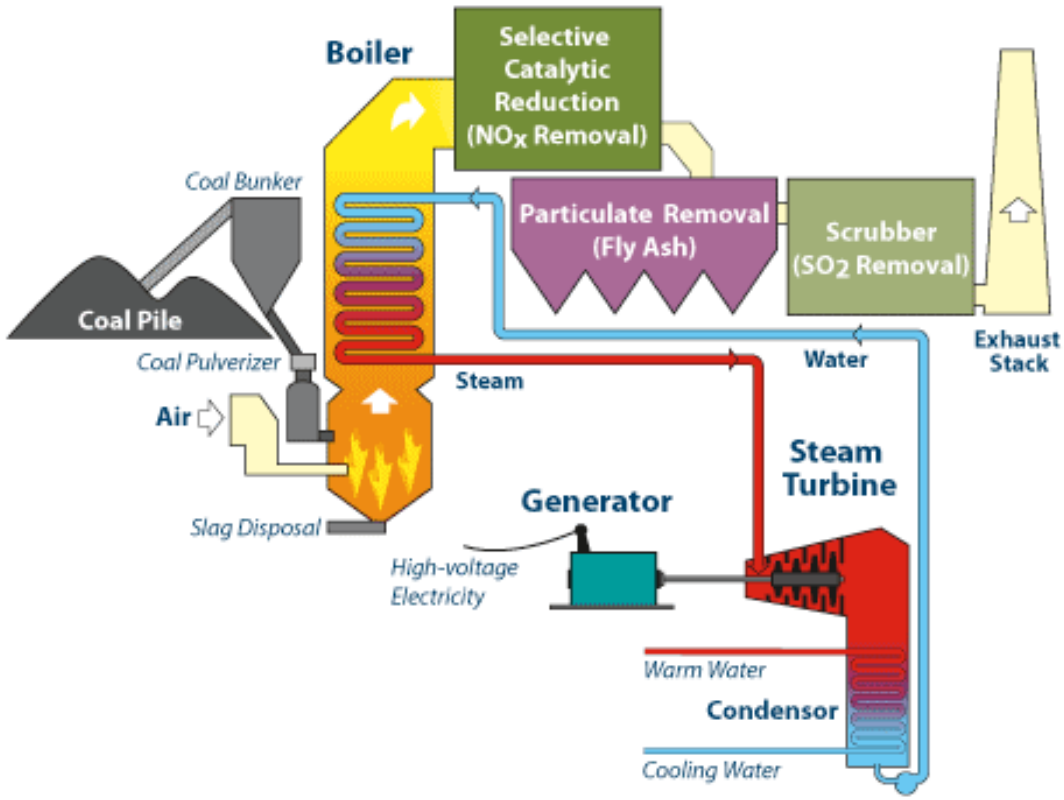

Highly Demanding Operating Conditions for Fe

Strengthening Mechanism	Effective Temperature
Work Hardening	~0.3 T_m
Grain Size	~0.3 T_m
Solid Solution Strengthening	~0.4 T_m
Precipitation Strengthening	~0.6 T_m
Oxide Dispersion Strengthening	~0.9 T_m

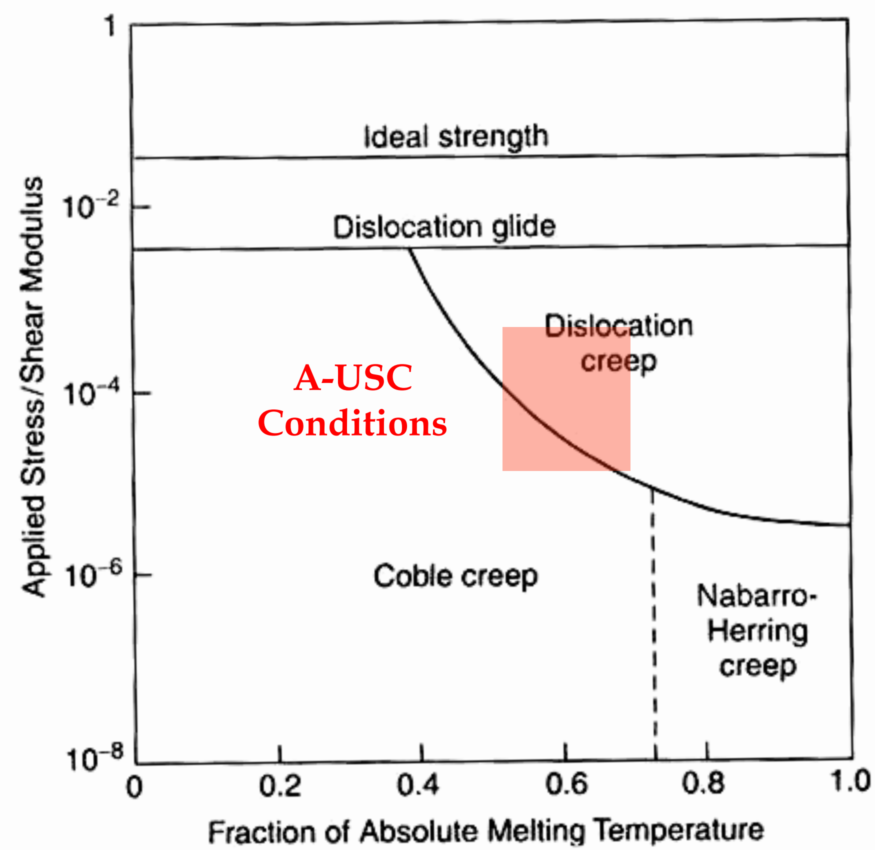

- **Oxide dispersion strengthening is best option for elevated temperature microstructure stability and creep resistance of Fe-base alloys**

Dislocation Substructure

- **TMT can be used to develop a dislocation substructure for increased alloy strengthening**
- **Sub-grain stability is highly dependent on the spatial distribution of the dispersoids**
- **Critical balance between driving and dragging forces (Zener pinning)**

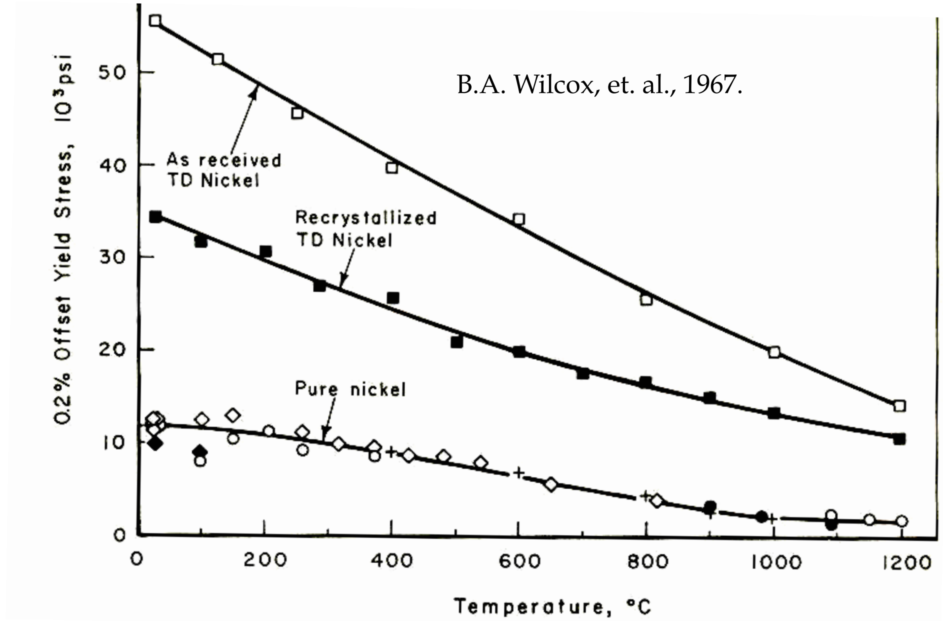

MA-956

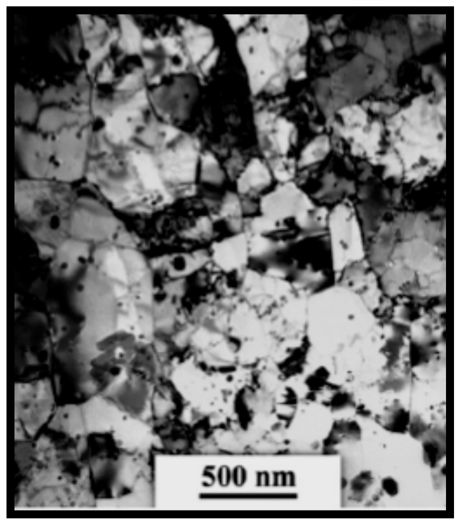

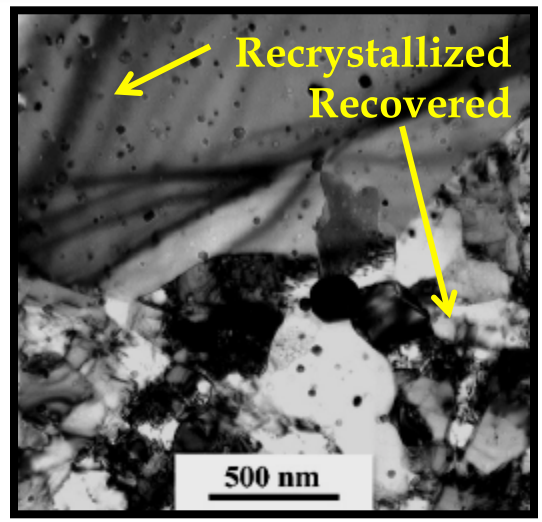

M.F. Hupalo, et al., 2004.

Fe-Based ODS Processing Comparison

* **Mechanical Alloying**

- **Long milling times**
- **Batch commercial process (< 2000 kg)**
- **Powder contamination (C, O, N, Ar)**
- **Anisotropic microstructure**

**

Gas Atomization (RSP)

- **Higher processing rates (10-20 kg/min)**
- **Continuous processing capacity**
- **Minimized contamination**
- **Isotropic microstructure capability**

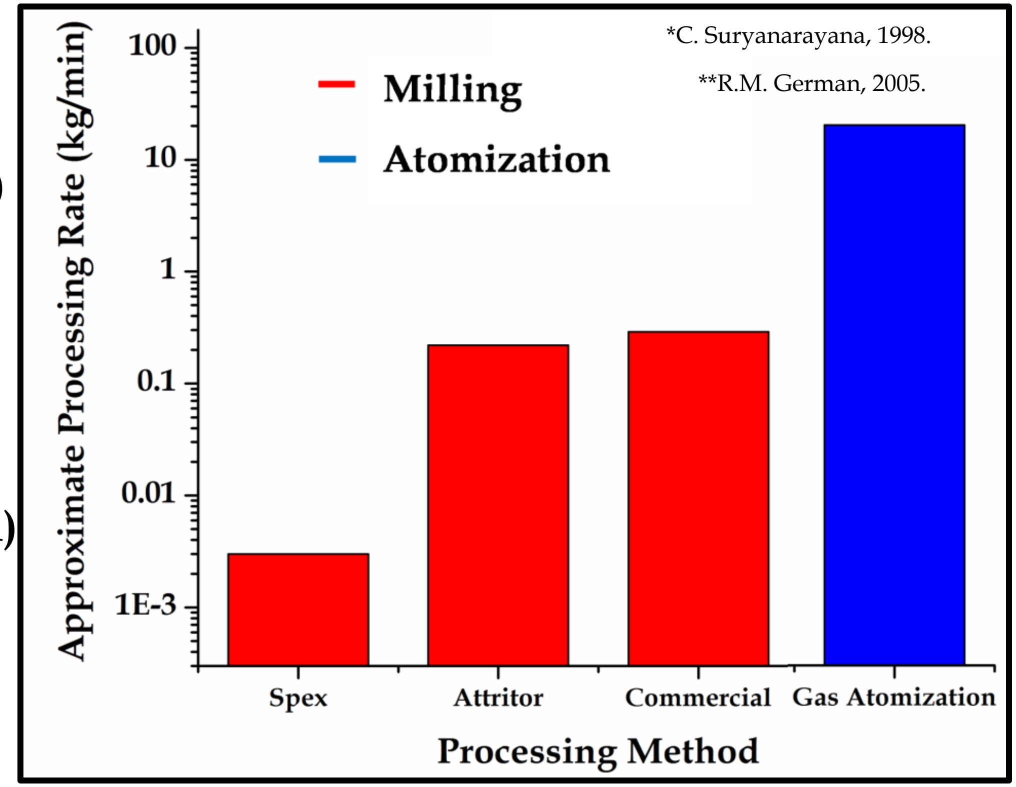

Material	Cost/kg (USD)	Notes
Ferritic Stainless Steel	~$2-5	446 Plate form
Fe-based ODS	~$165, ~$345	MA956 Sheet (Special Metals), PM 2000 (Plansee)
Ni-based	~$30-35	Inconel 718 Sheet (Special Metals), Inconel 617 (Special Metals)

ODS Processing Cost!

Gas Atomization Reaction Synthesis

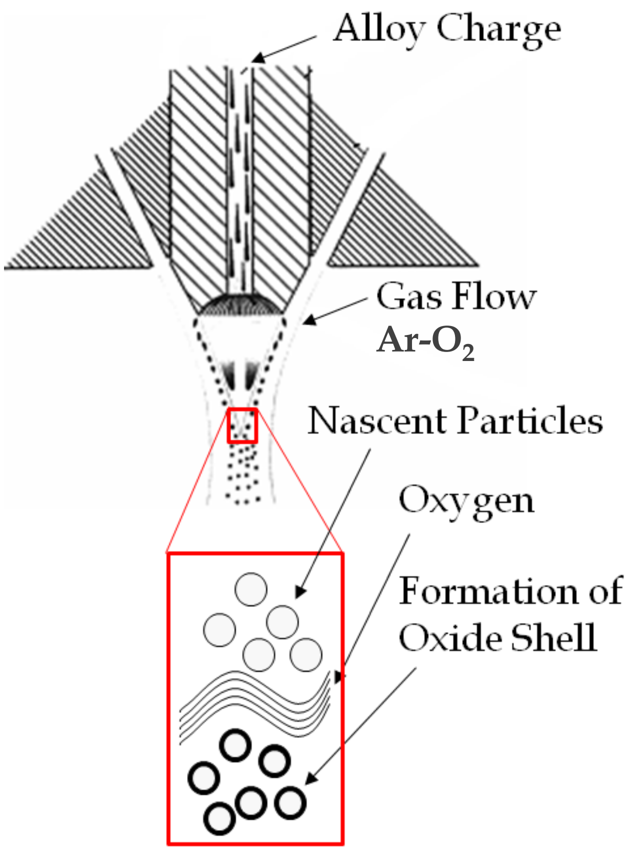

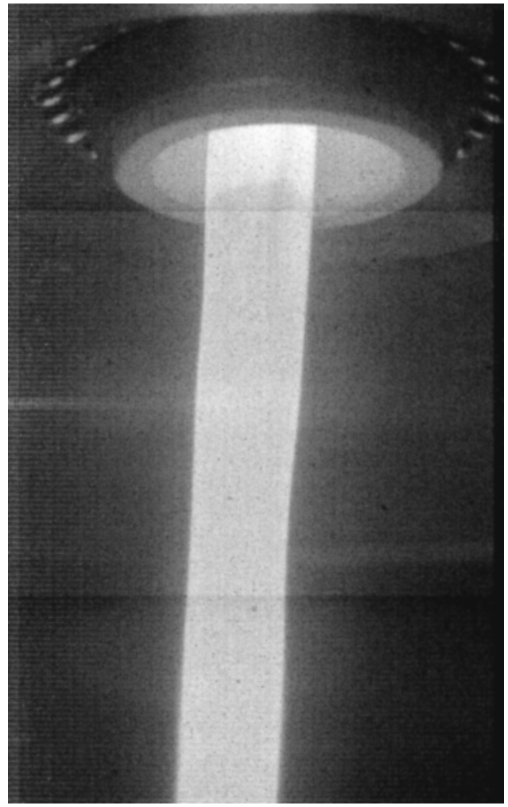

~0.1 sec.

Alloy Element	Primary Function
Cr	Surface reactant Oxidation resistance
Y	Dispersoid former
Ti	Surface reactant Dispersoid stabilizer
Hf	Surface reactant Dispersoid stabilizer
O	Surface oxidant Dispersoid former

In situ alloying addition of oxygen (primarily) as transient powder surface oxide.

Chemical Reservoir Alloy Design

Internal Oxygen Exchange Reaction

- **Y-enriched intermetallic compound (IMC) precipitation (Y reservoir)**
- Dissociation of Cr-enriched prior particle boundary (PPB) oxide (O reservoir)

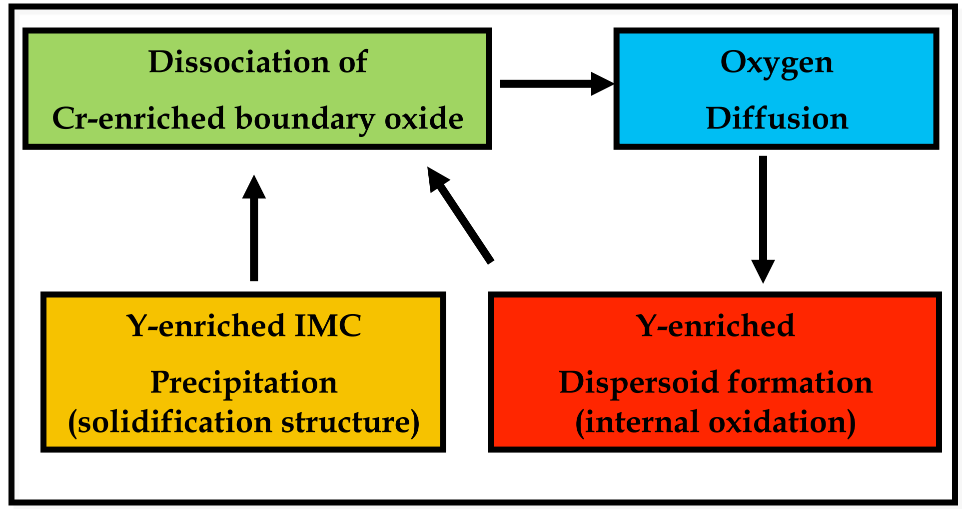

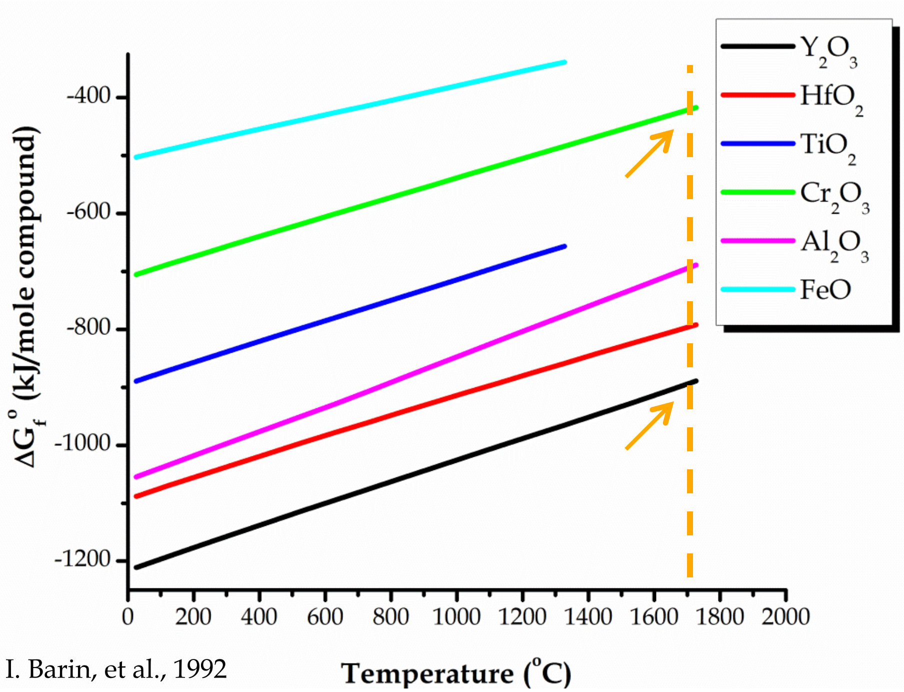

I. Barin, et al., 1992

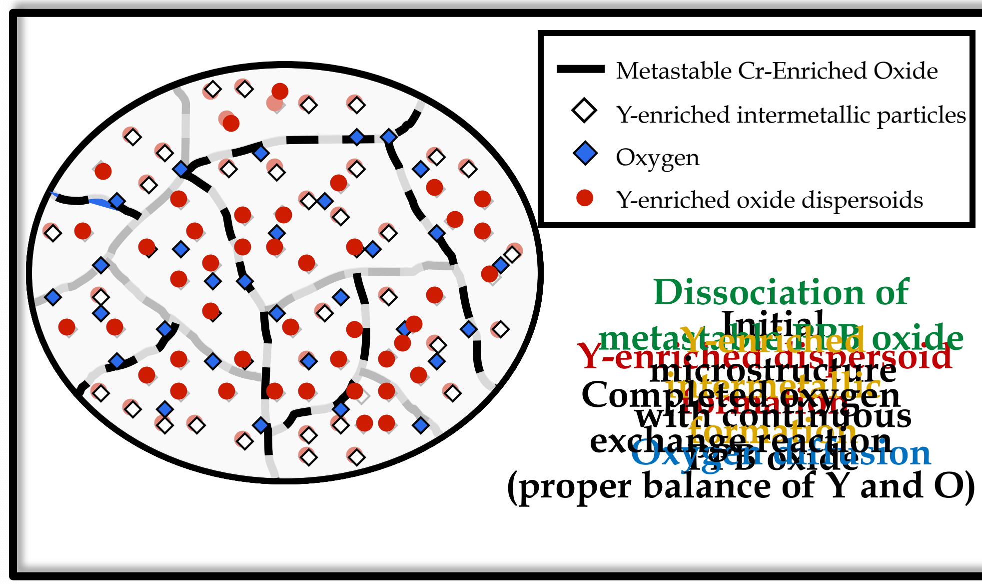

Chemical Reservoir Phase Evolution

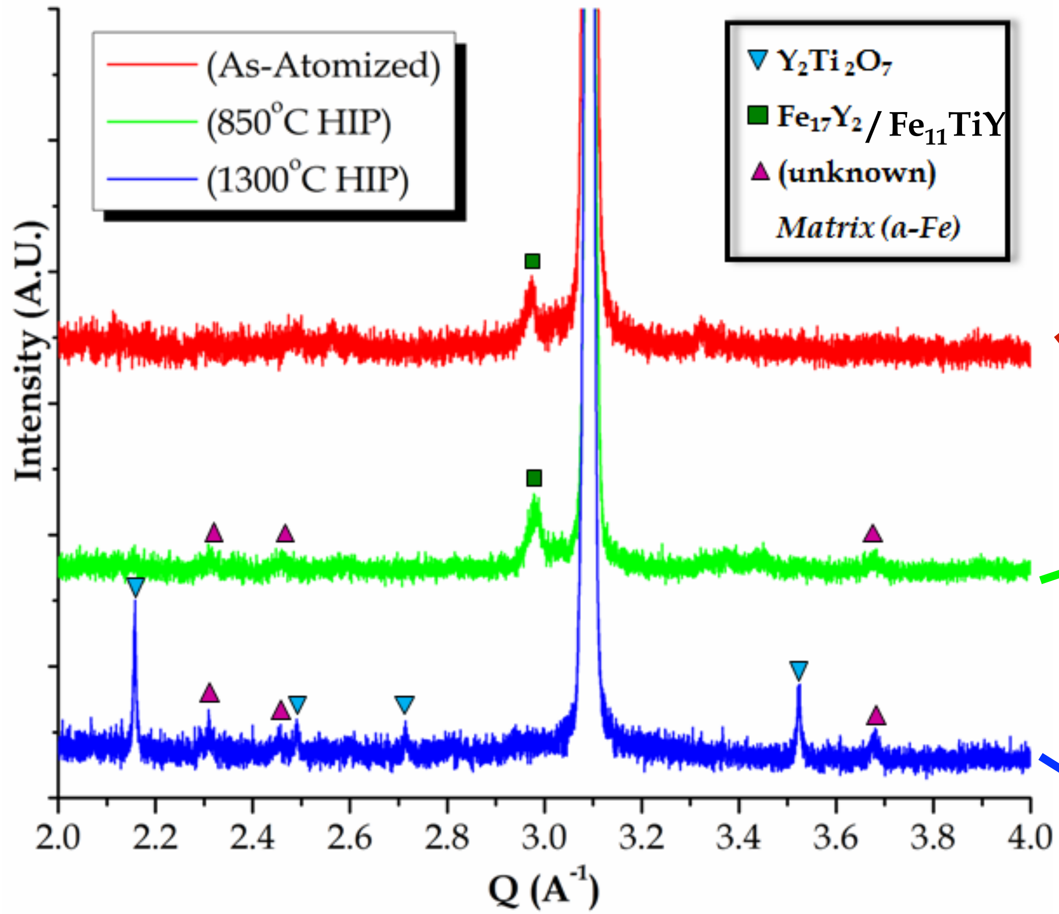

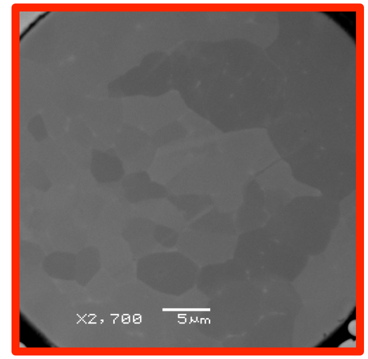

As-Atomized Powder

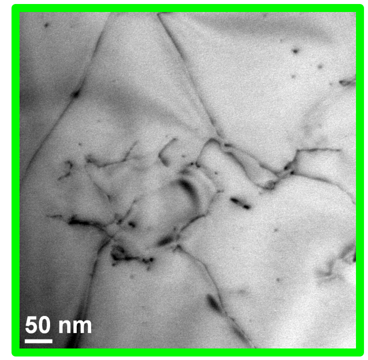

HIP Consolidation 850°C

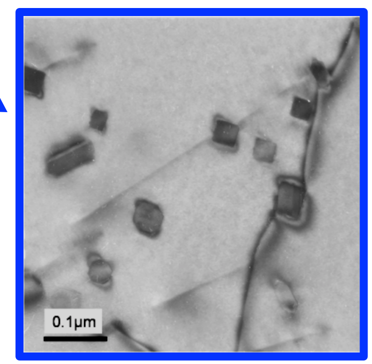

HIP Consolidation 1300°C

~1.0 vol. % Dispersoid

PPB Oxide	IMC Precipitates	Matrix Phase	Nano-metric Dispersoids

$$Cr_2O_3 + Fe_{11}TiY \longrightarrow (Fe, Cr)_{ss} + Y_2Ti_2O_7$$

Fe-15.70Cr-0.20Y-0.49Ti-1.16O (at%)

GARS Process Control

Resulting Oxygen Content Control Approach

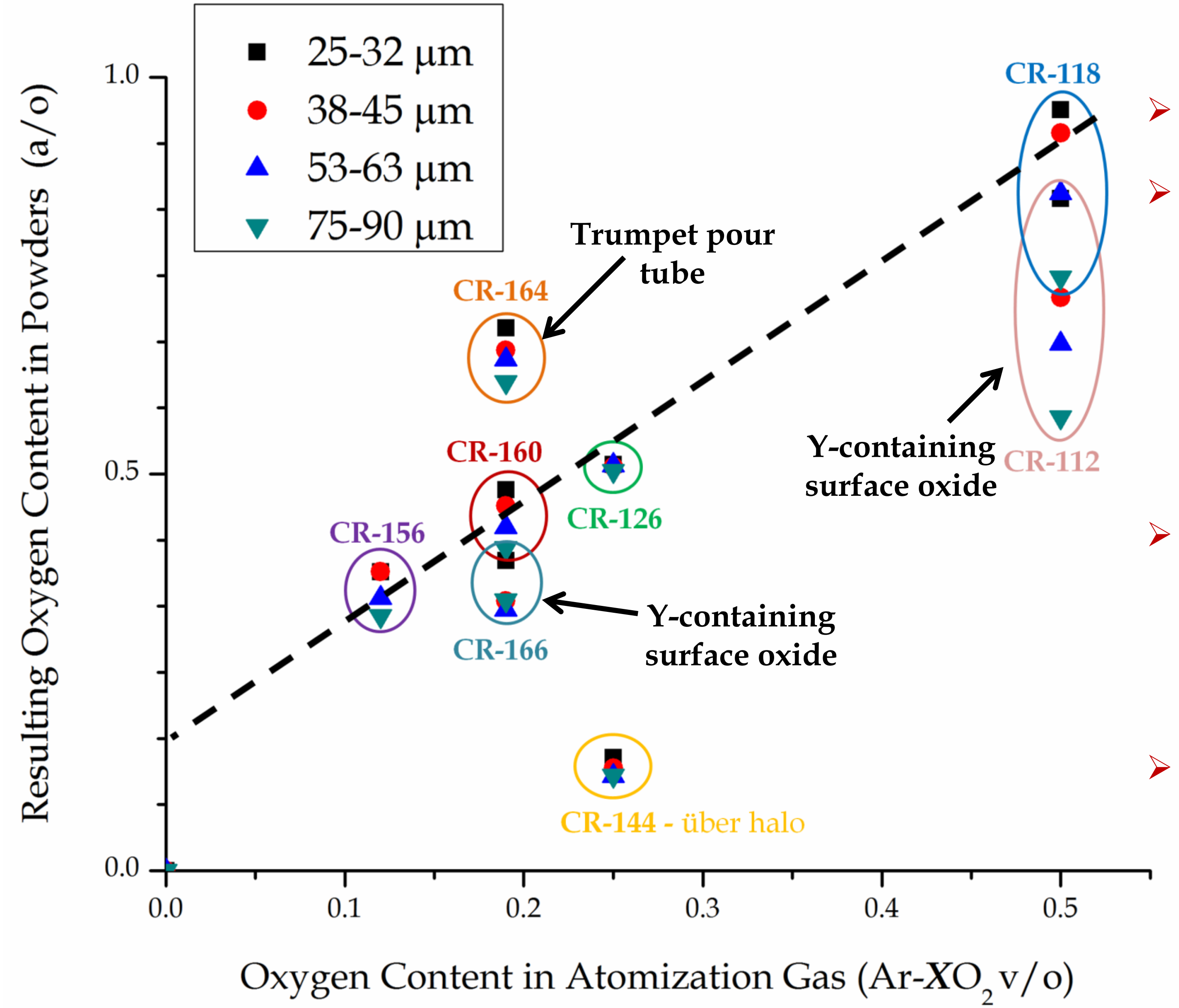

- **Rapid oxidation kinetics**
- **Empirically determined linear oxidation dependence on p_{O_2}**

$$k_p \propto (P_{O_2})^{\frac{1}{n}}$$

Where, n =1

- **Decreased oxidation kinetics when Y present in the surface oxide layer**

E.J. Felten, 1991.

- **Sensitive to atomization processing parameters (i.e., gas nozzle and pour tube design)**

Surface Oxide Analysis (AES)

CR-156Y-Hf: Fe-15.84Cr-0.11Hf-0.18Y at.%

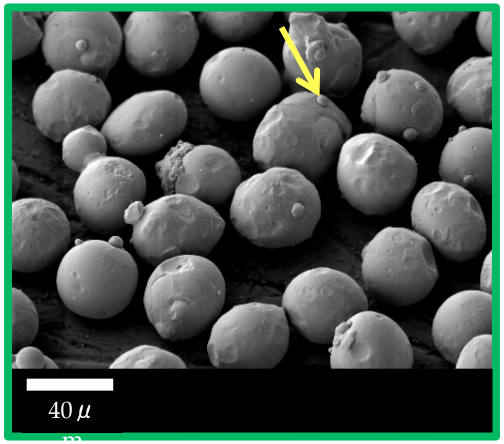

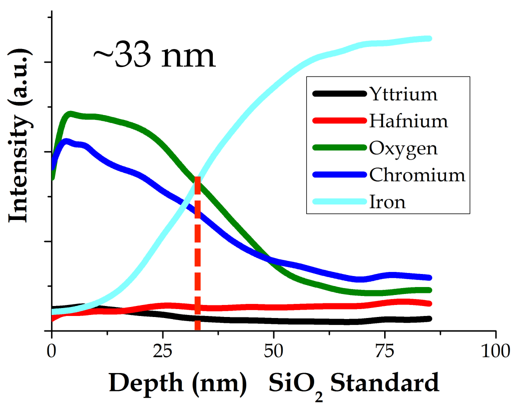

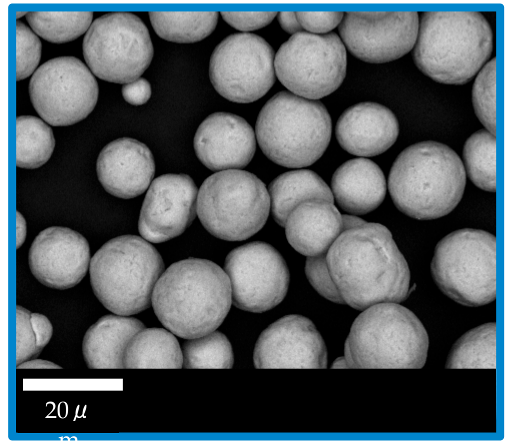

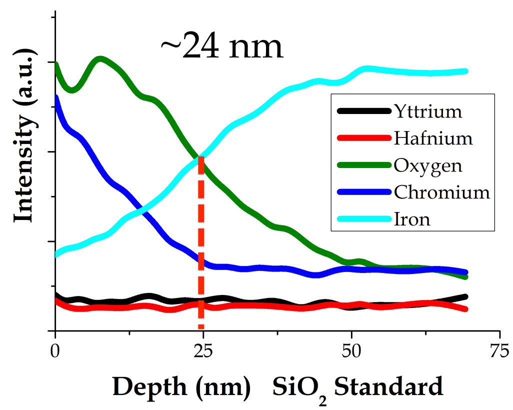

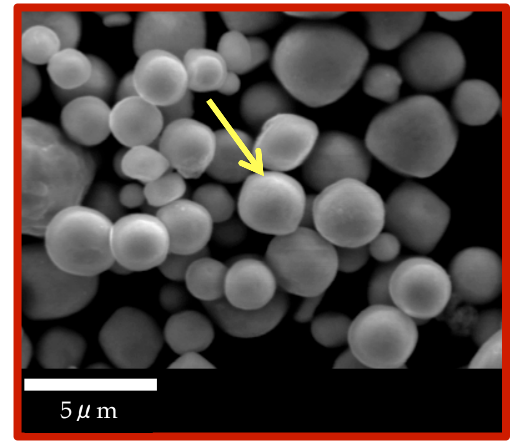

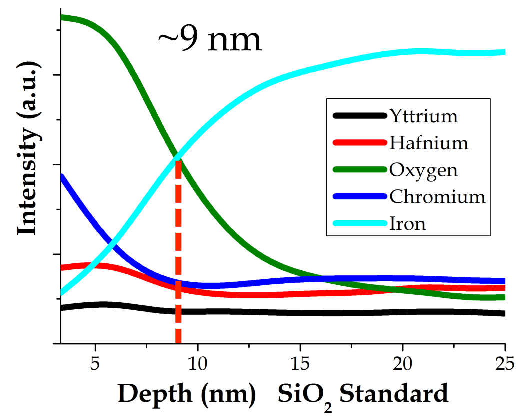

Decreasing particle size

Decreased surface oxidation

Resulting Surface Oxide Layer Thickness

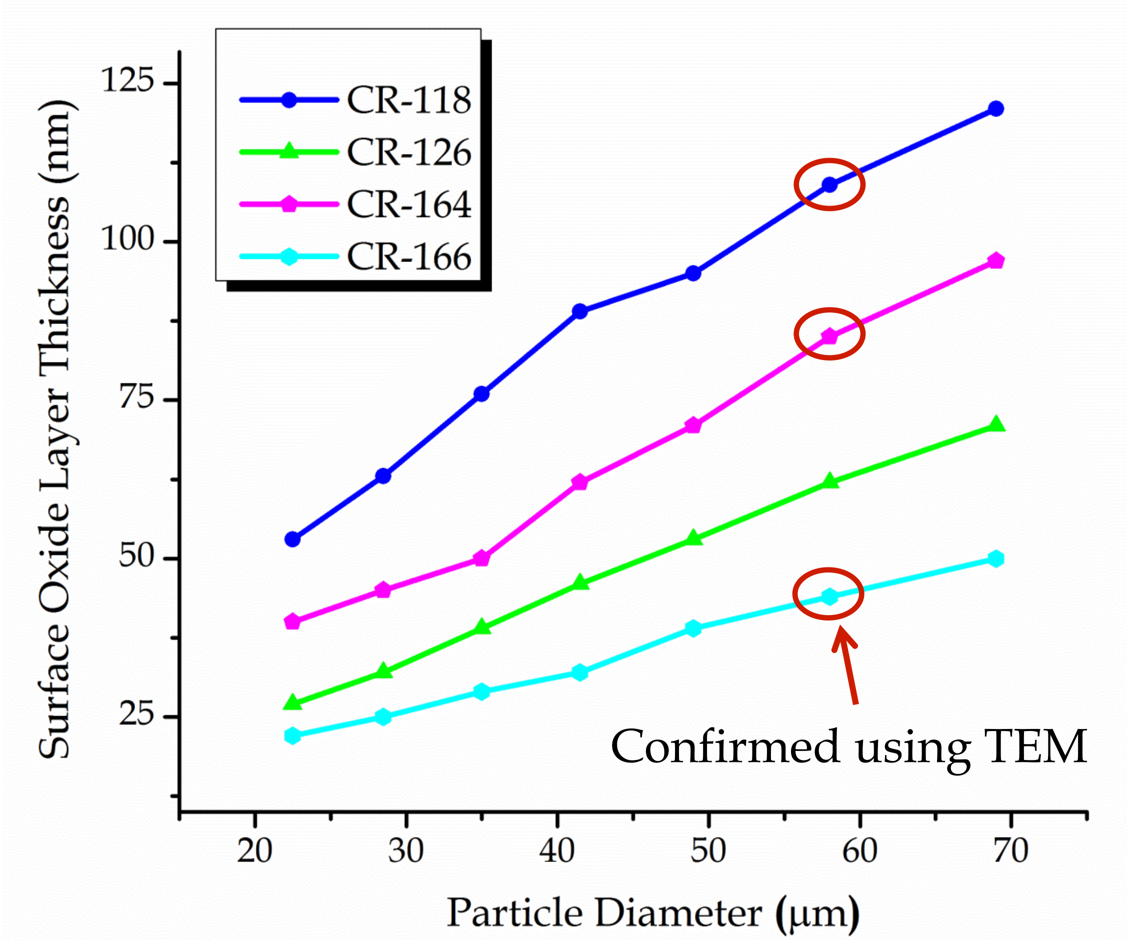

Assumptions

- All oxygen is in the form of a uniform surface oxide layer
- Cr_2O_3 surface oxide formation

$$\xi_{ox} = \frac{\Delta m_{O_2} W_{ox}}{S_d W_{O_2} y \rho_{ox}}$$

Where, $M_a O_y$

-Kubaschewski, et al. 1962.

- **Why is there a particle size dependence?**

Predicted Oxide Layer Thickness

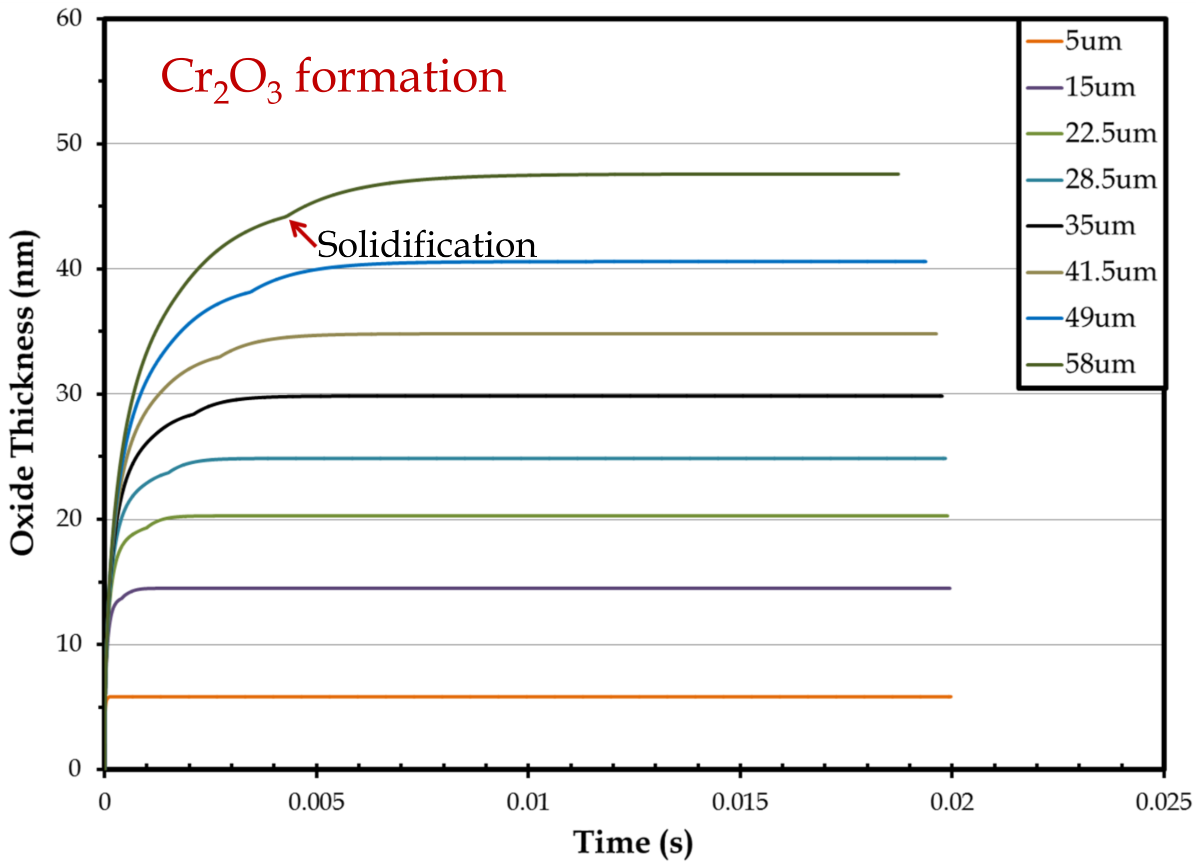

- Utilizing the droplet cooling curves (T vs. t)
- Oxidation reaction deemed complete when $\delta < 400$ nm sec^{-1}
- Majority of oxidation occurs prior to droplet solidification

Parabolic Oxidation Rate Constant

$$k_p = B\exp\left(\frac{-E}{RT}\right)$$

Where, E=249kJ/mol (Gulbransen et al., 1957)

B=5 $g^2cm^{-4}s^{-1}$ (experimental)

$$k_p \propto (P_{O_2})^{\frac{1}{n}} \quad n=1 \text{ (experimental)}$$

Oxygen Mass Gained

$$\Delta m_{O_2}(\Delta t) = \left(\frac{k_{p,i} + k_{p,f}}{2}\right)^{\frac{1}{2}} \cdot 2S_d\left(t_f^{\frac{1}{2}} - t_i^{\frac{1}{2}}\right)$$

Resulting Oxide Layer Thickness

$$\xi_{ox} = \frac{\Delta m_{O_2} W_{ox}}{S_d W_{O_2} y \rho_{ox}}$$

Oxide Growth

$$\delta = \frac{\Delta \xi_{ox}}{\Delta t}$$

Comparison with Experimental Results

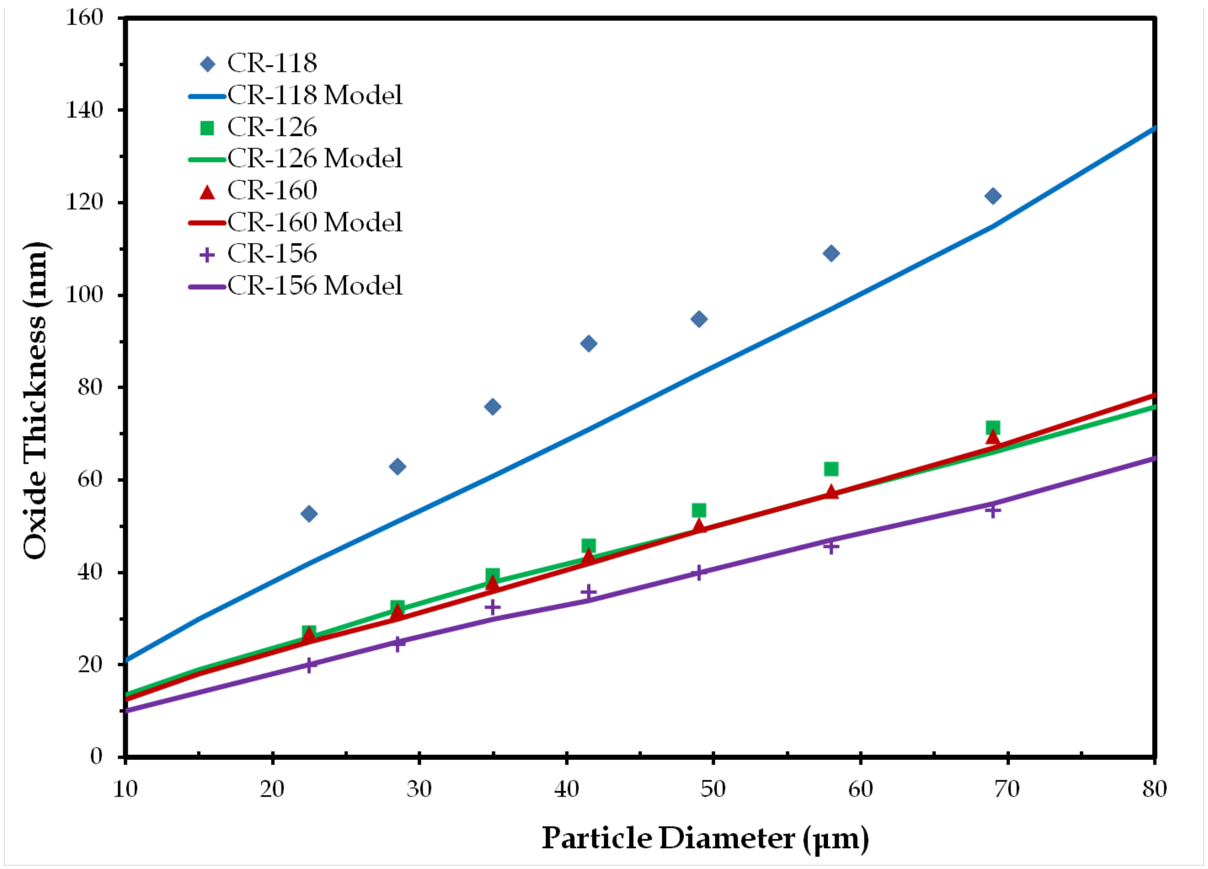

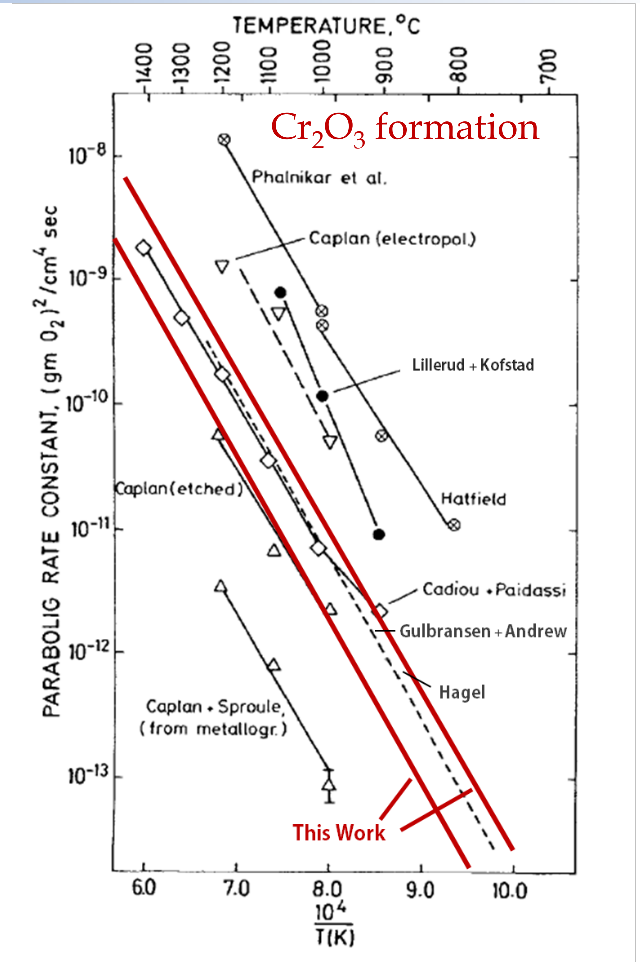

- Initially optimized for CR-118 (parabolic oxidation pre-factor)
- Modified atomization processing parameters and ran model for each similar CR-alloy
- **Recommended as a processing tool to predict and control *in situ* O additions during atomization**

ODS Microstructure Control

As-Atomized Solidification Structure

CR-156Y-Hf: Fe-15.84Cr-0.11Hf-0.18Y at.%

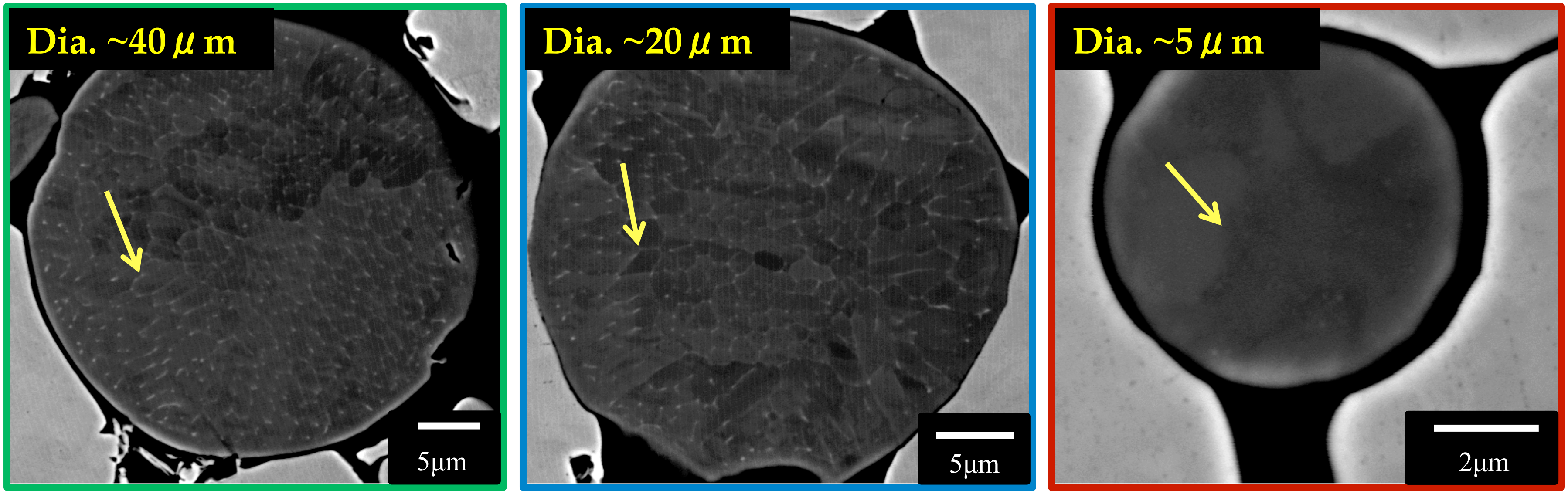

- Microsegregation observed in coarser powders
- Apparent solute trapping in ultra-fine (dia. < 5μm) powders
- APT highlighted intermetallic clusters

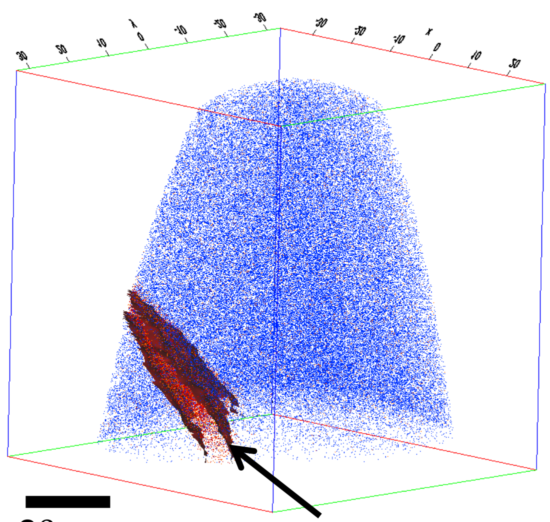

Fe-(Y,Hf) Precipitate

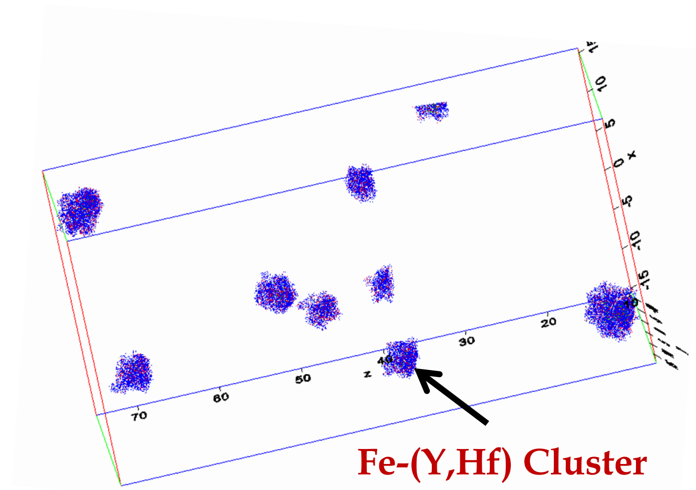

Fe-(Y,Hf) Cluster
Size: 2-5 nm
No. Density: 2-6x 10^{22} m^{-3}

Calculated Solidification Velocity

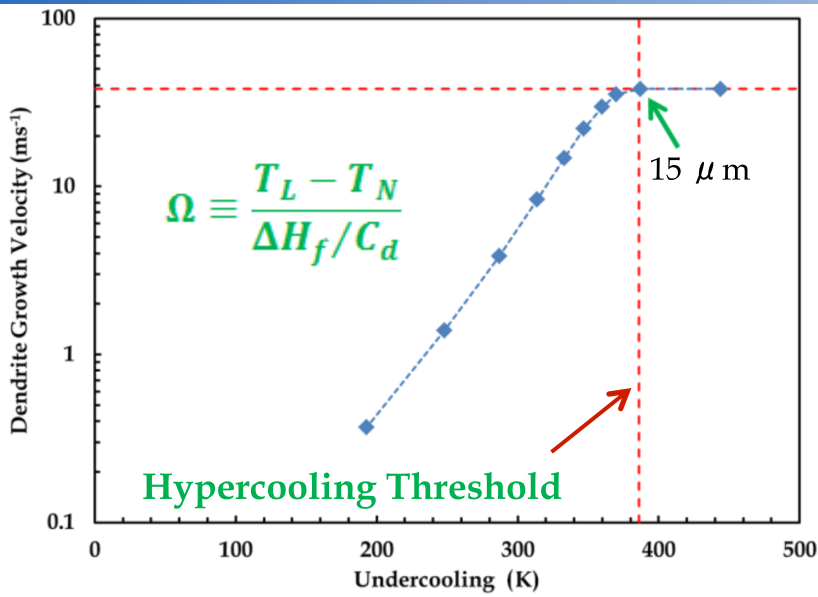

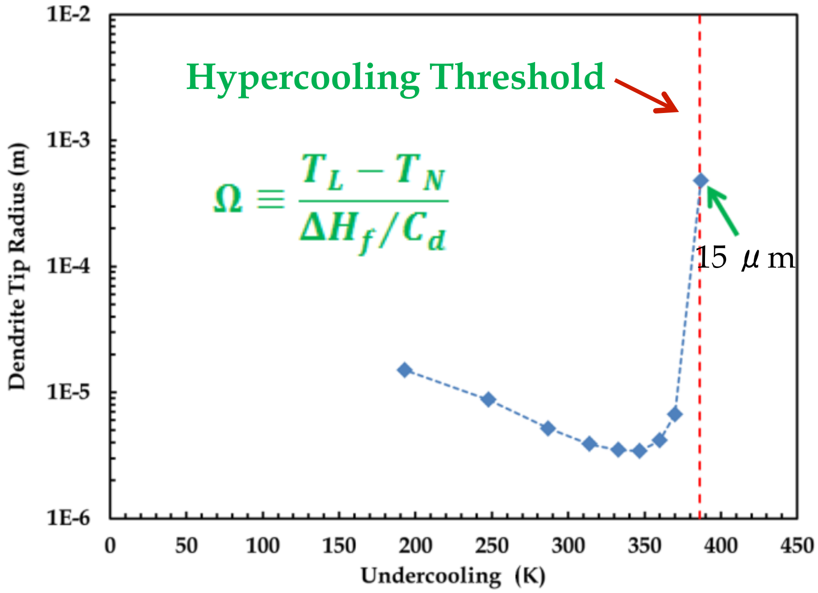

Approximation of the Invanstov Function

$$Pe_t = a\left(\frac{\Omega}{1-\Omega}\right)^b$$ (Wang et al., 1993)

Truncated LKT Model

$$r_{den} = \frac{\Gamma/\tau^*}{(\Delta H_f/C_d)Pe_t(1-n)}$$

$$V_{den} = \frac{2Pe_t\alpha}{r_{den}}$$

(Lipton, Kurz, and Trivedi, 1987)

Planar Stability, when $\Omega \geq 1$

$$(V_{den})_{abs} = \frac{\alpha_L \Delta H_f}{\Gamma C_{d,L}}$$

(Trivedi and Kurz, 1986)

Calculated Solidification Velocity

CR-156Y-Hf: Fe-15.84Cr-0.11Hf-0.18Y at.%

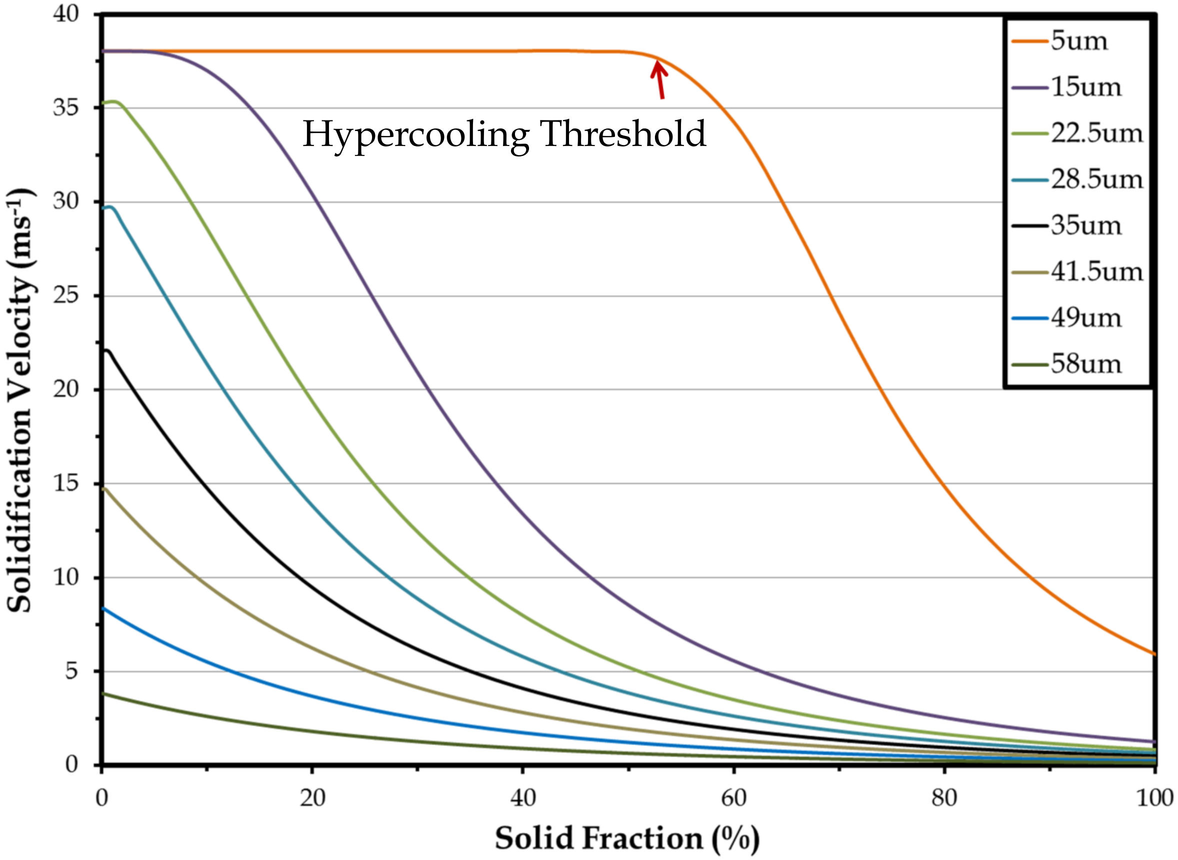

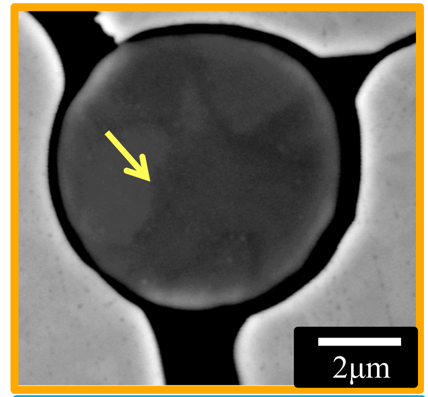

Solute Trapping!

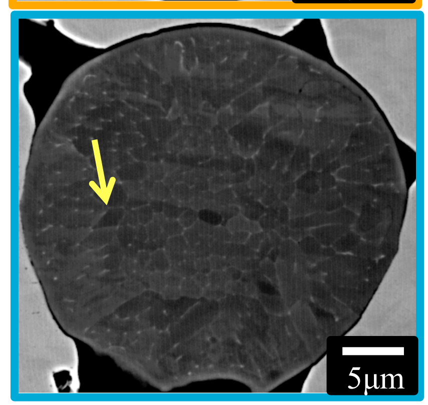

Micro-segregation

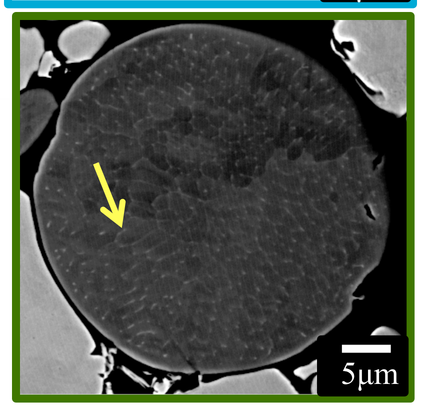

Micro-segregation

Planar (microsegregation-free) growth

$$(V_{den})_{abs} = \frac{\alpha_L \Delta H_f}{\Gamma C_{d,L}} \quad \text{(Trivedi and Kurz, 1986)}$$

$$Q_{re} = \Delta H_f V_{den} A_d \rho_d$$

Precursor IMC Precipitate Distribution

CR-156Y-Hf: Fe-15.84Cr-0.11Hf-0.18Y at.%

<u>As-HIPed 700°C – 300MPa – 4hr</u>

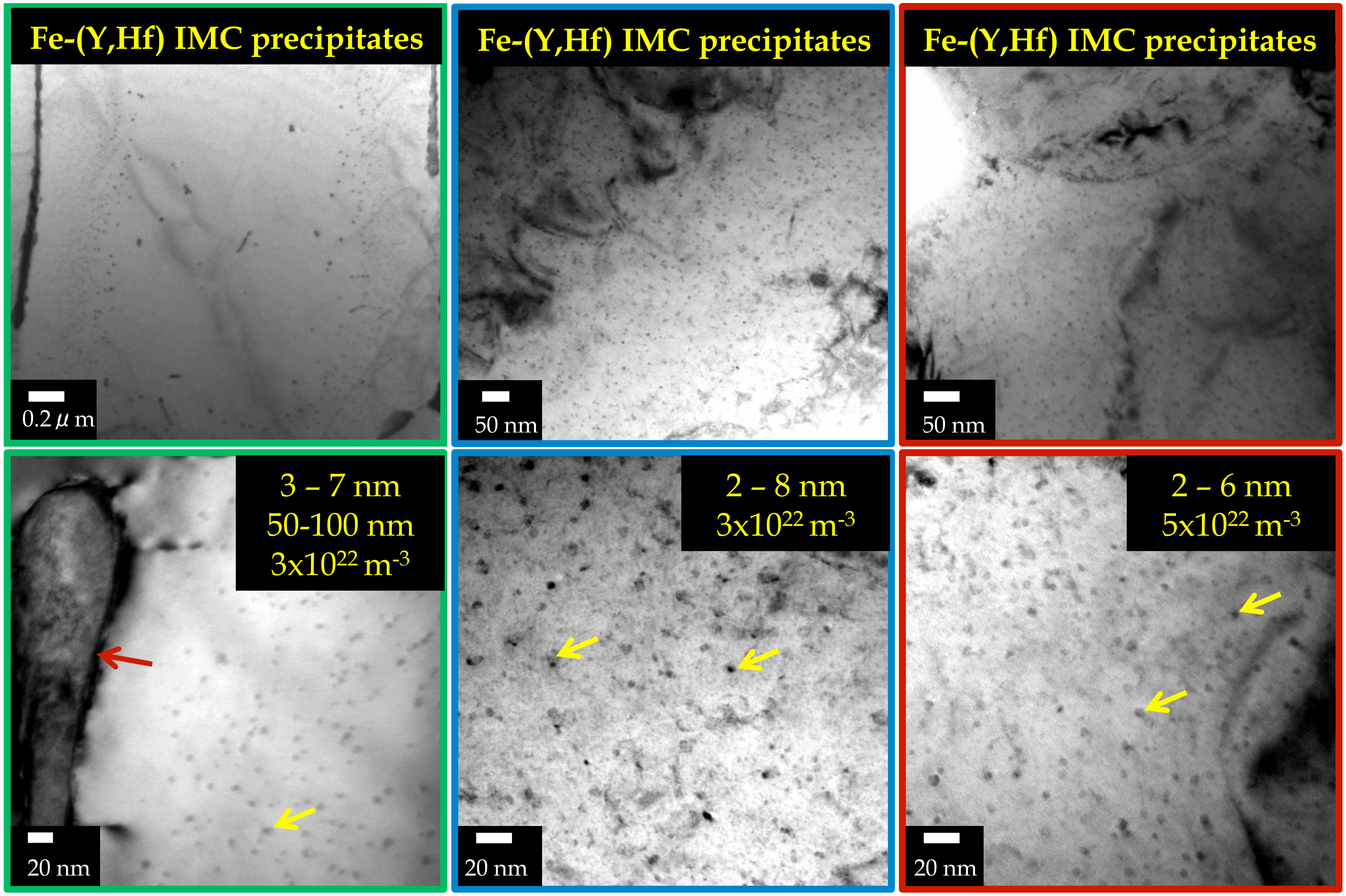

Dia. 20-53 μm | **Dia. 5-20 μm** | **Dia. < 5 μm**

Resulting ODS microstructure

CR-156Y-Hf: Fe-15.84Cr-0.11Hf-0.18Y at.%

Heat Treated 1200°C – 2.5hr – Vac.

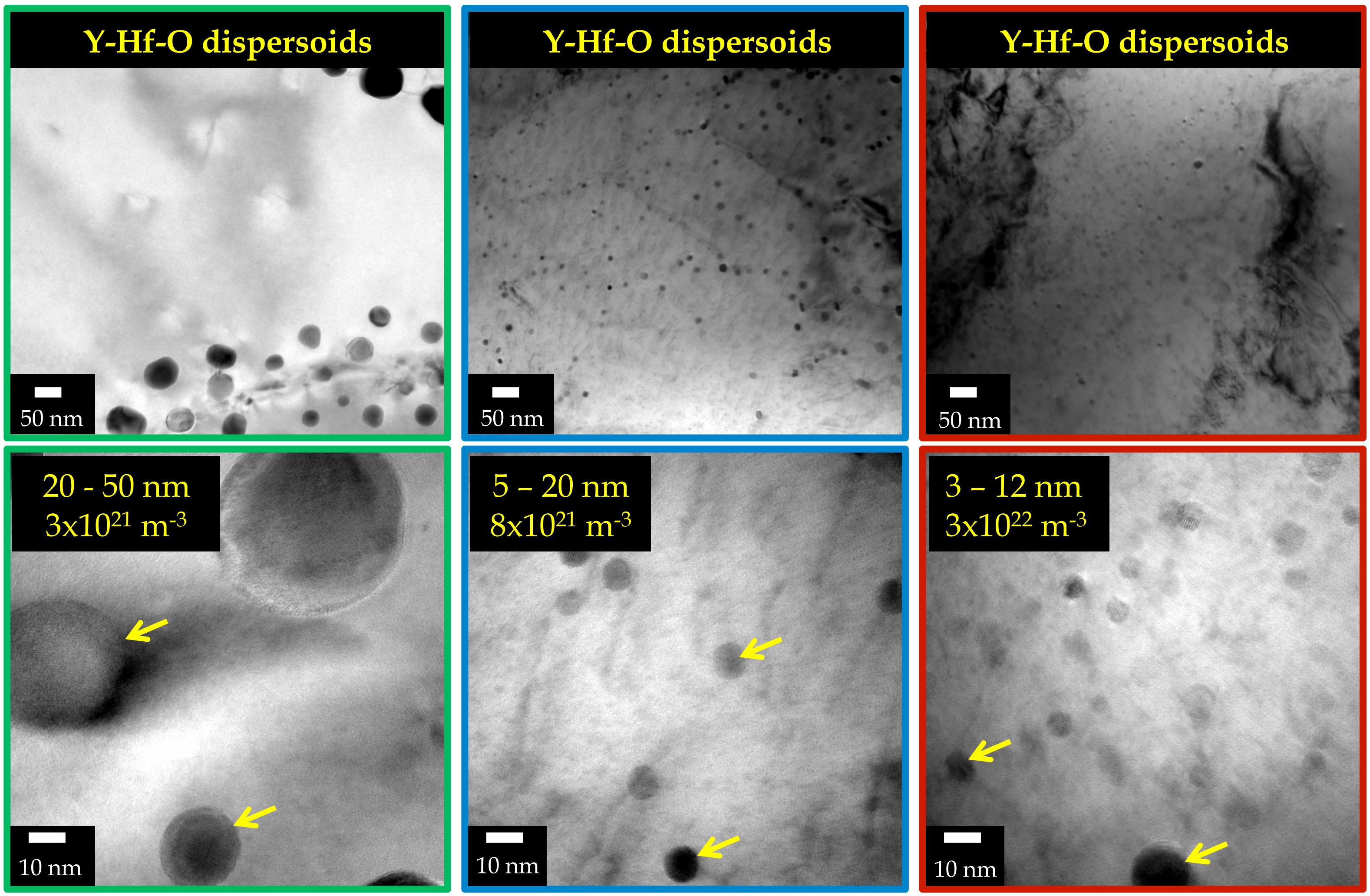

Dia. 20-53 μ m | **Dia. 5-20 μ m** | **Dia. < 5 μ m**

Thermal Mechanical Treatment

ODS Microstructure

CR-166 (< 20 μ m): Fe-15.91Cr-0.12Ti-0.09Y-0.49O at.%

CR-166 (45-75μm): Fe-15.91Cr-0.12Ti-0.09Y-0.33O at.%

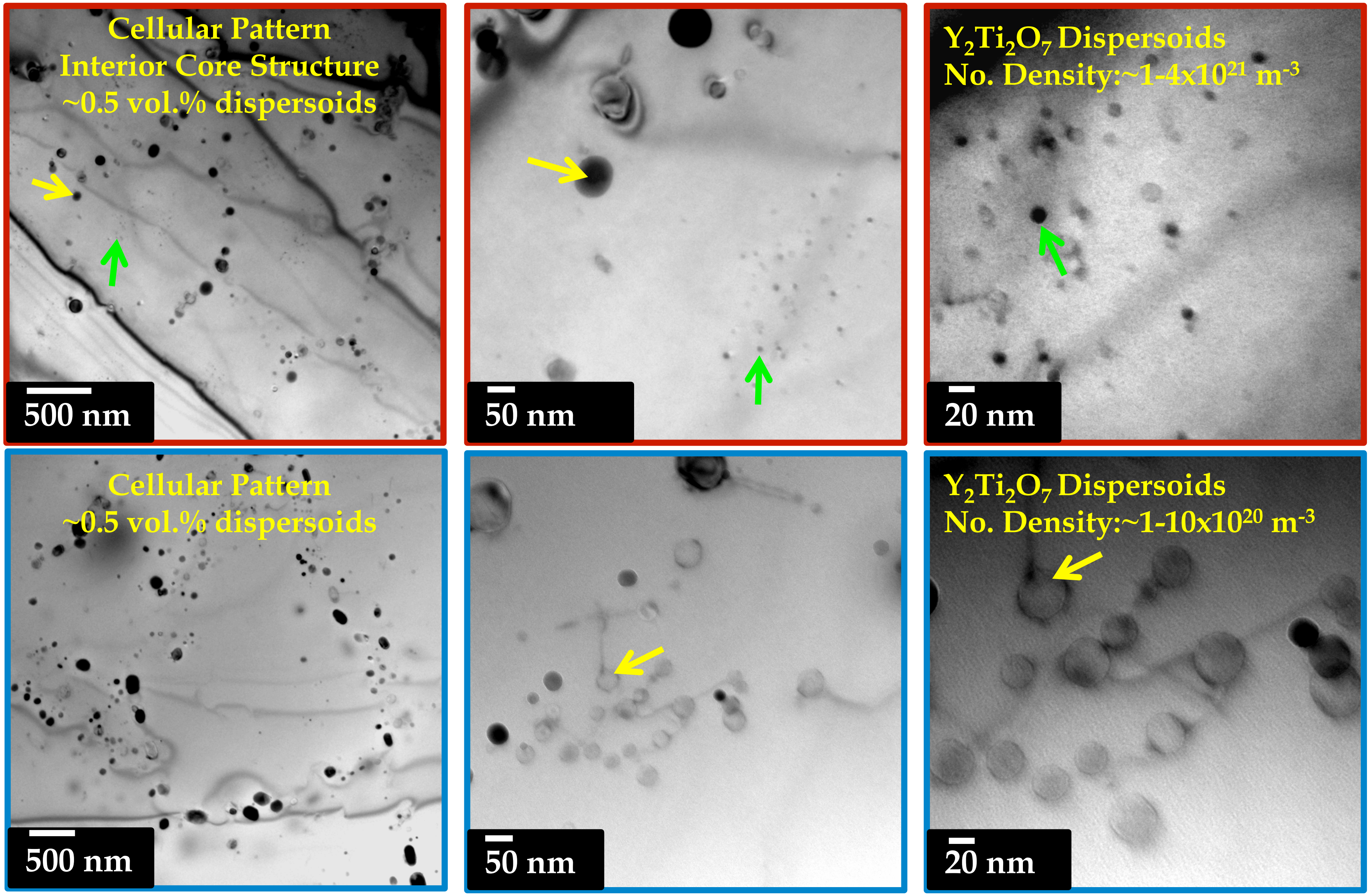

The Ames Laboratory
Creating Materials & Energy Solutions
U.S. DEPARTMENT OF ENERGY

U.S. DEPARTMENT OF ENERGY

IOWA STATE UNIVERSITY
OF SCIENCE AND TECHNOLOGY

Cold Rolled Microhardness

CR-166 (< 20 μ m): Fe-15.91Cr-0.12Ti-0.09Y-0.49O at.%
CR-166 (45-75μm): Fe-15.91Cr-0.12Ti-0.09Y-0.33O at.%

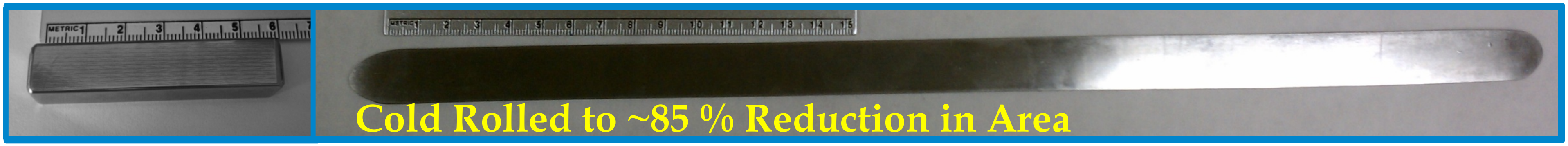

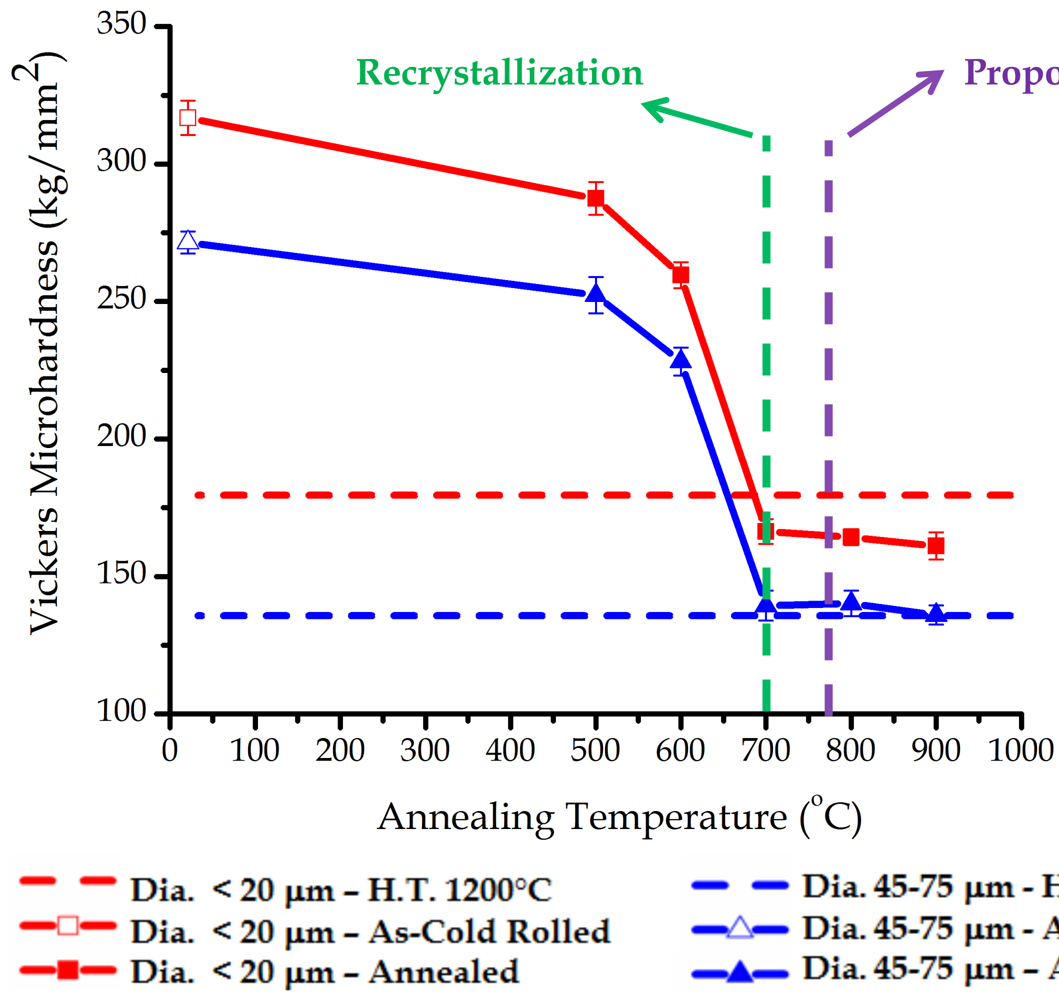

- ~2X increase in microhardness
- Cold work threshold
- Microstructure dependent (Zener Limit)

Annealed Microstructure

CR-166 (< 20 μm): Fe-15.91Cr-0.12Ti-0.09Y-0.49O at.%
CR-166 (45-75μm): Fe-15.91Cr-0.12Ti-0.09Y-0.33O at.%

Heat Treated 1200°C | Cold Rolled 85% RA + Annealed 500°C-1hr-Air | Cold Rolled 85% RA + Annealed 500°C-1hr-Air + 800°C-1hr-Air

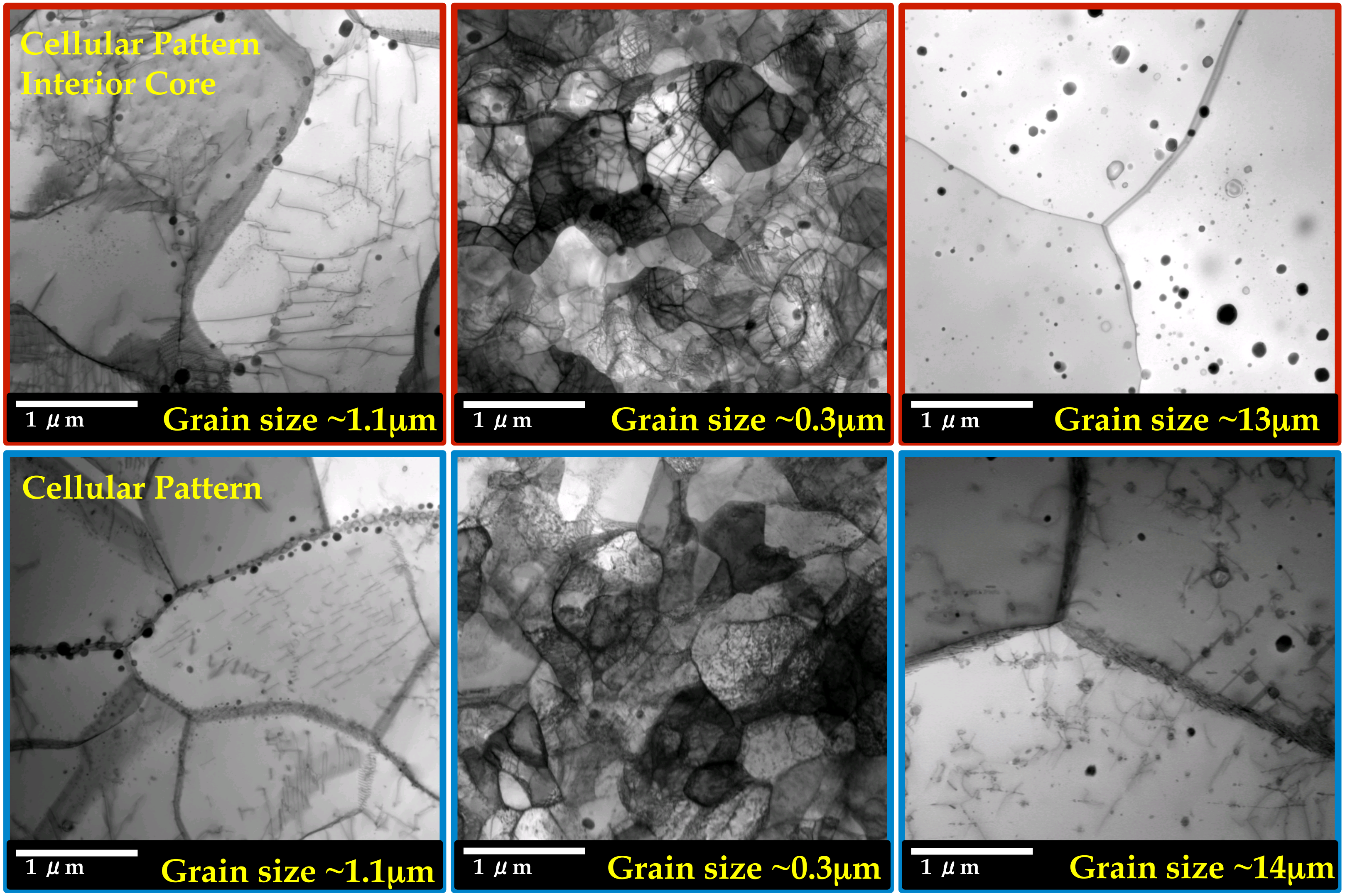

Mechanical Properties

CR-166 (< 20 μ m): Fe-15.91Cr-0.12Ti-0.09Y-0.49O at.%
CR-166 (45-75μm): Fe-15.91Cr-0.12Ti-0.09Y-0.33O at.%

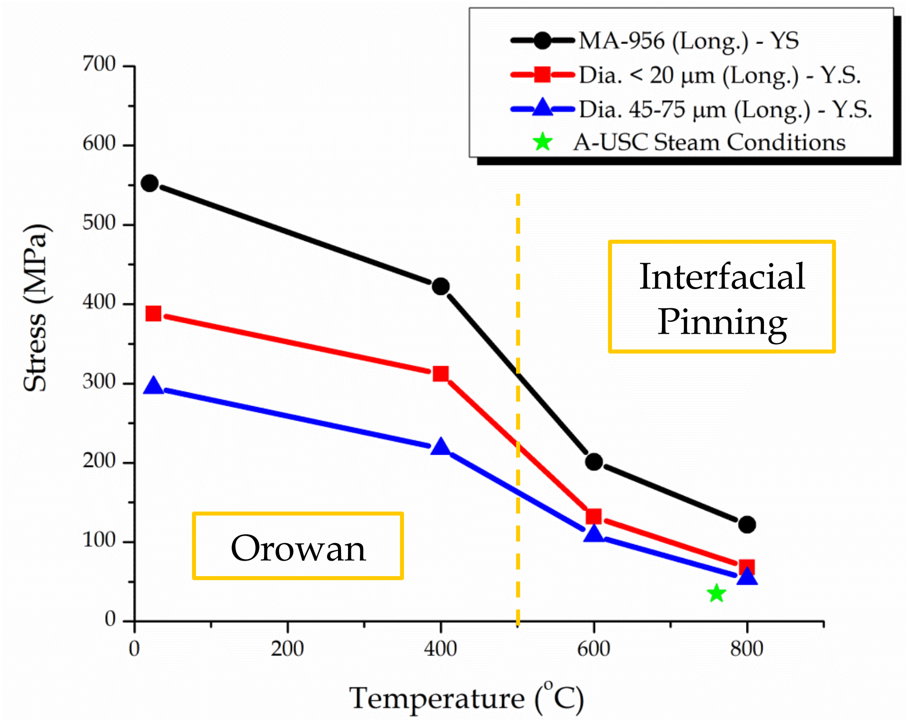

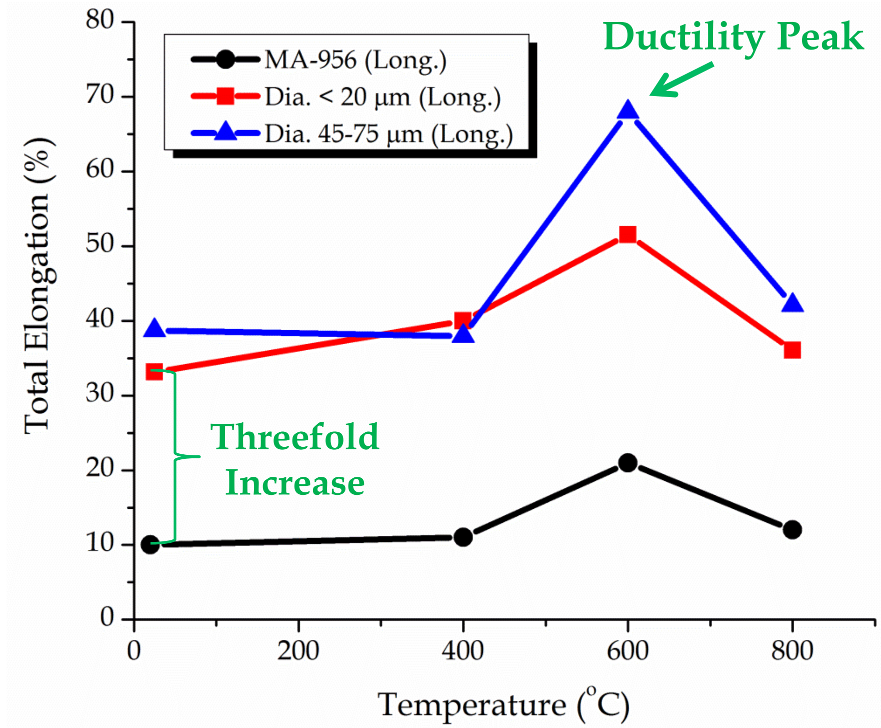

- **Mean free path for dislocation movement (Orowan)**
- **Dislocation climb and detachment stress (interfacial pinning)**
- **A threefold increase in total elongation**

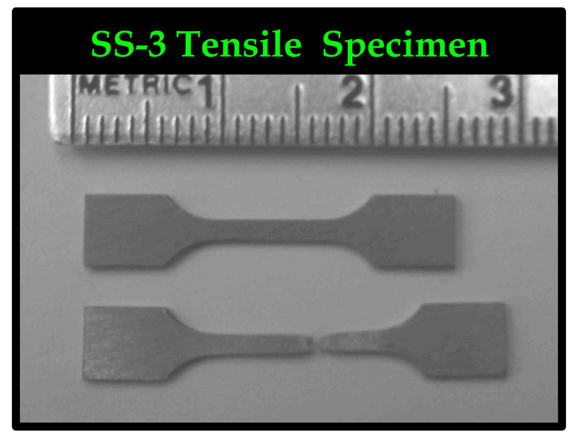

Thermal Stability

Thermal Stability (1200°C)

CR-164HfY: Fe-15.55Cr-0.12Hf-0.09Y-1.04O at.%
CR-166TiY: Fe-15.91Cr-0.12Ti-0.09Y-0.49O at.%

1200°C 2.5 hr | **1200°C 100 hr** | **1200°C 1,000 hr**

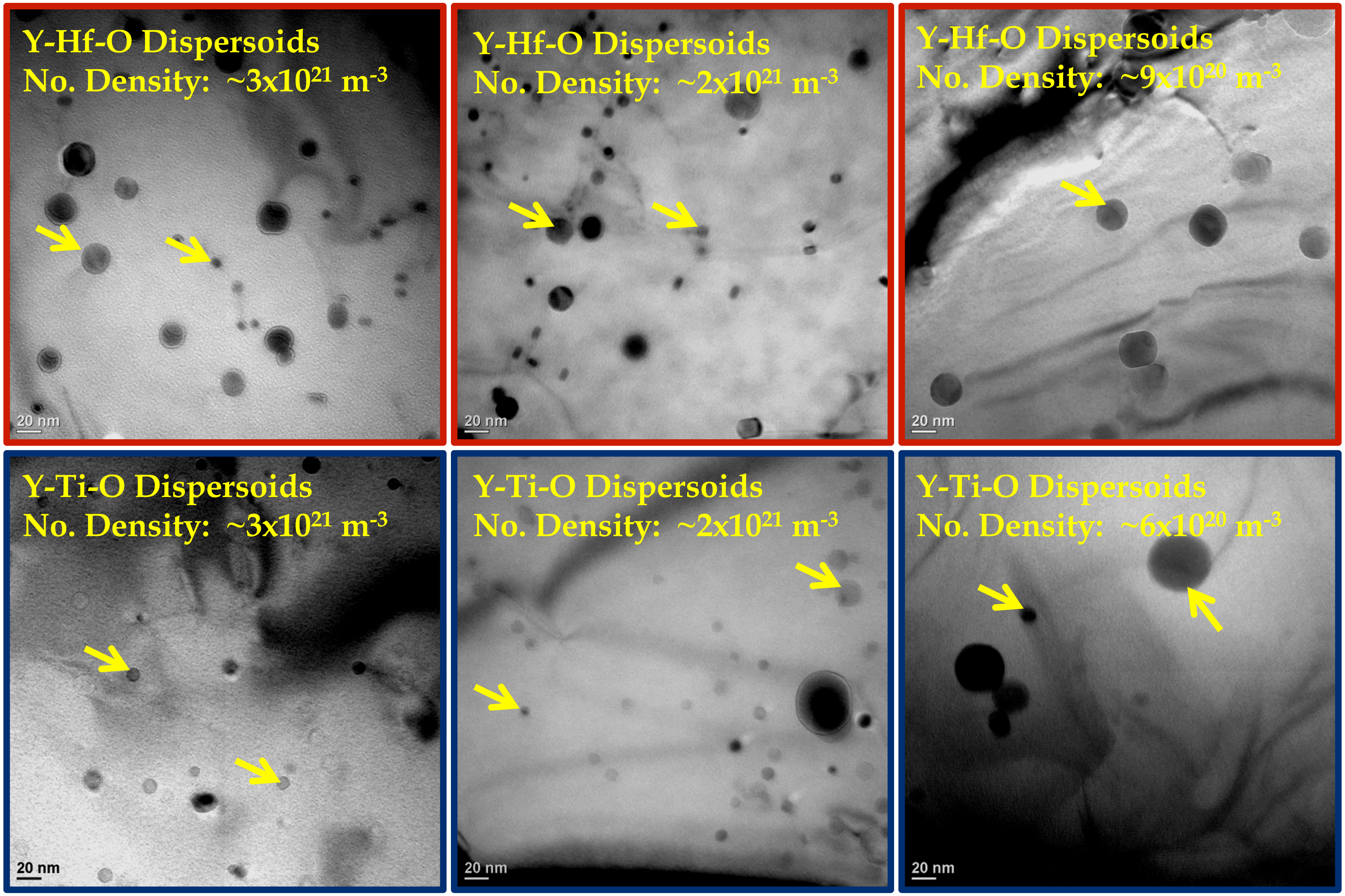

Microstructure Evolution

CR-164HfY: Fe-15.55Cr-0.12Hf-0.09Y-1.04O at.%
CR-166TiY: Fe-15.91Cr-0.12Ti-0.09Y-0.49O at.%

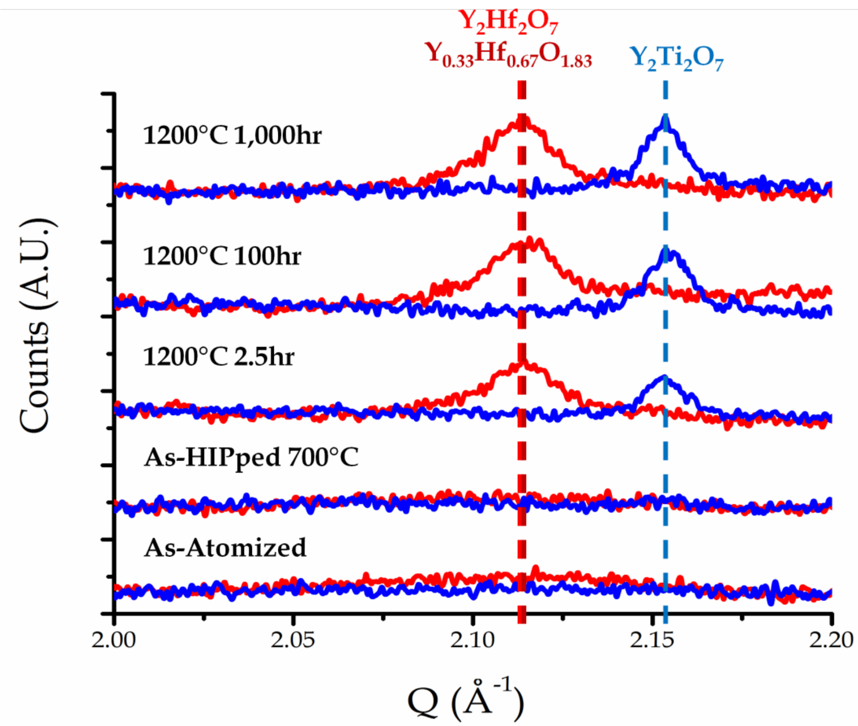

Time at 1200°C (hrs)	CR-164HfY Calc. Radius (nm)	CR-166TiY Calc. Radius (nm)
2.5	11.7	19.2
100	11.9	19.8
1,000	12.9	22.0

$$t \approx \frac{k\lambda}{\beta \cos\theta_\beta}$$ (B.D. Cullity, 1967)

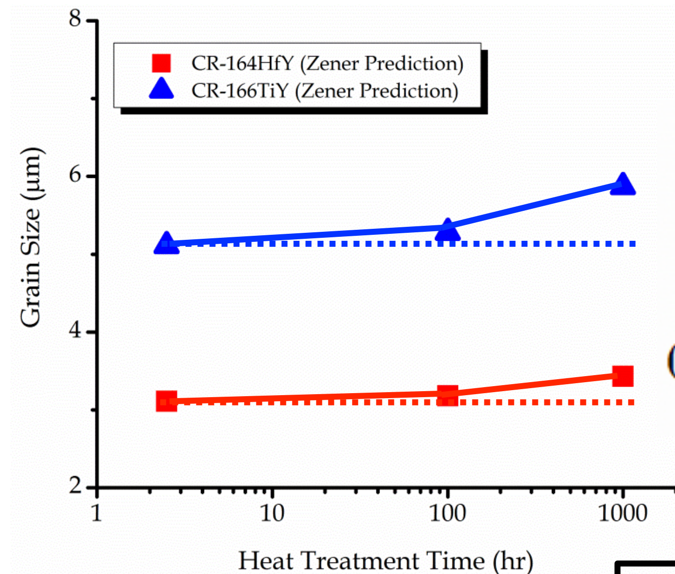

$$R_c = \frac{4r}{3f}$$

Zener Pinning

(C.S. Smith, 1948)

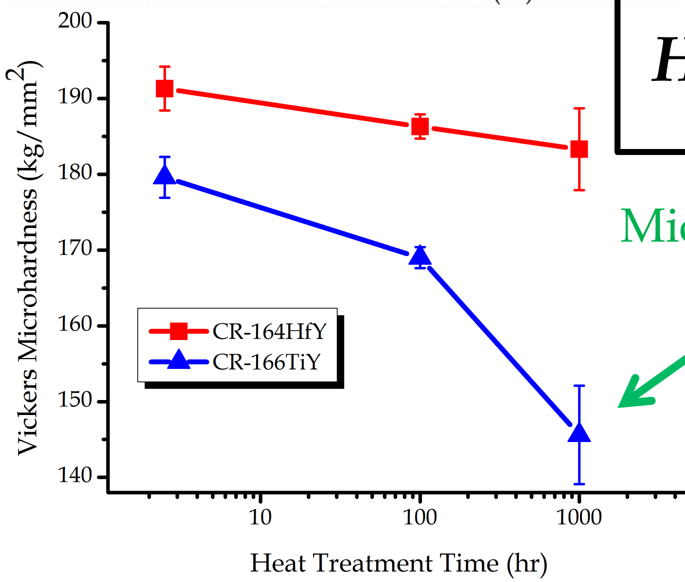

Hf vs. Ti

Microhardness drop

Future Work

New Fe-based ODS atomization trial

GARS Process Control	
Composition	Fe-16Cr-0.30Hf-0.20Y-0.70O at.%
Size Range Goal	Dia. < 10μm
Reaction Gas	Ar-0.06O_2 vol.%
Dispersoid Phase	$Y_2Hf_2O_7$
Atomization Parameters	
Nozzle	45° (closed wake)
Pressure	600 psi
Pour Tube	Super heating composite
Metal Flow Rate	1 kg/min

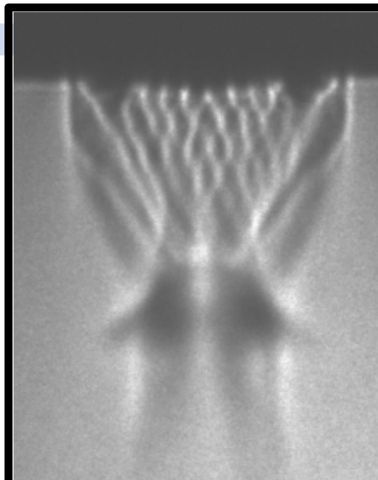

Focused Supersonic Gas Patterns

Close-Coupled HPGA

Superheat Pour Tube Module

Yttria Tungsten YSZ Final Part

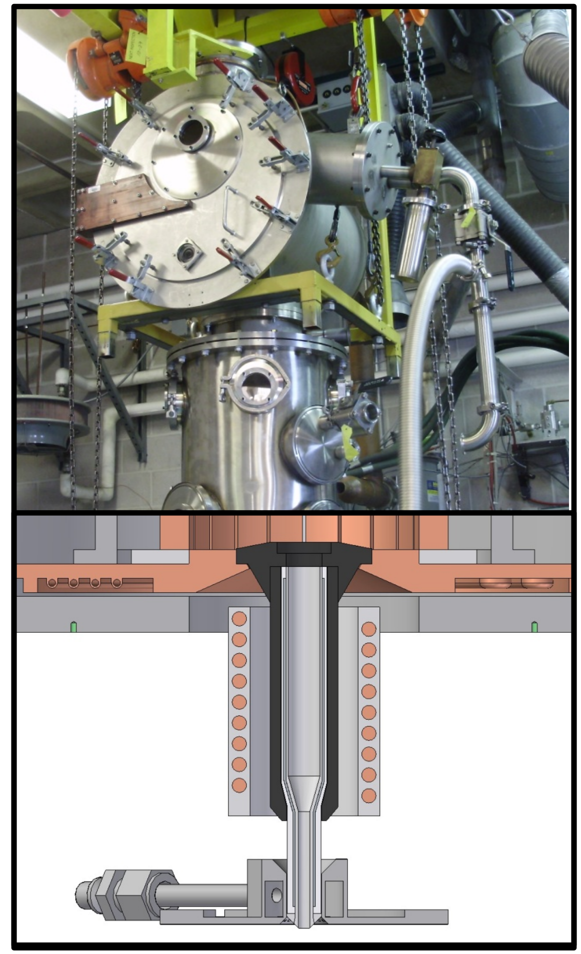

- **Efficiently add ~250°C of superheat to the molten alloy as it is transported from the crucible to the high pressure atomization gas**
- **Prevents "freeze-out" during atomization runs that utilize low metal flow rates**

ORNL Collaboration

Fe-16.8Cr-0.90W-0.62Ti-0.08Y-0.26O at.%
(Fe-15.1Cr-2.95W-0.53Ti-0.12Y-0.07O wt.%)

- ➢GARS Powders (GA-130TiY: Dia. < 20μm)
- ➢Ball Milled (5hr)
- ➢Loaded into HIP canister
- ➢Vacuum outgassed (415°C)
- ➢Seal HIP canister (E-beam weld)
- ➢HIP cycle: 850°C – 4hr – 300 MPa (Ar)
- ➢Remove canister and machine into bar
- ➢Thermal mechanical treatment (hot rolling)
- ➢Machine and test creep specimens at ORNL

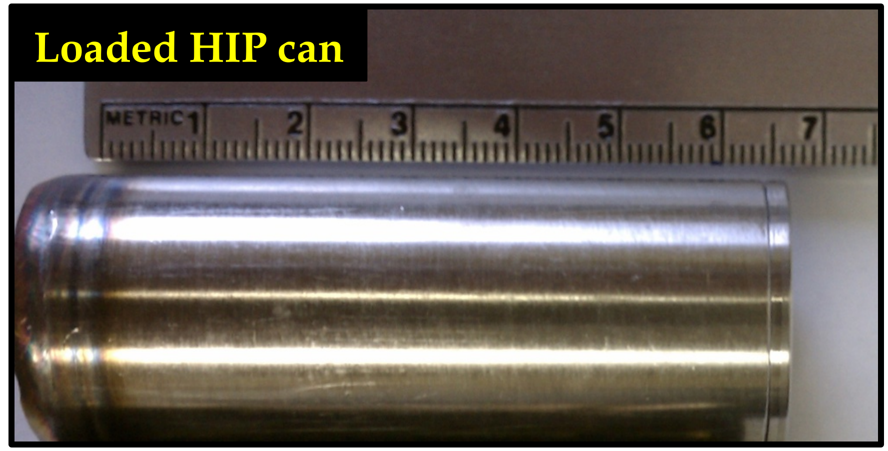

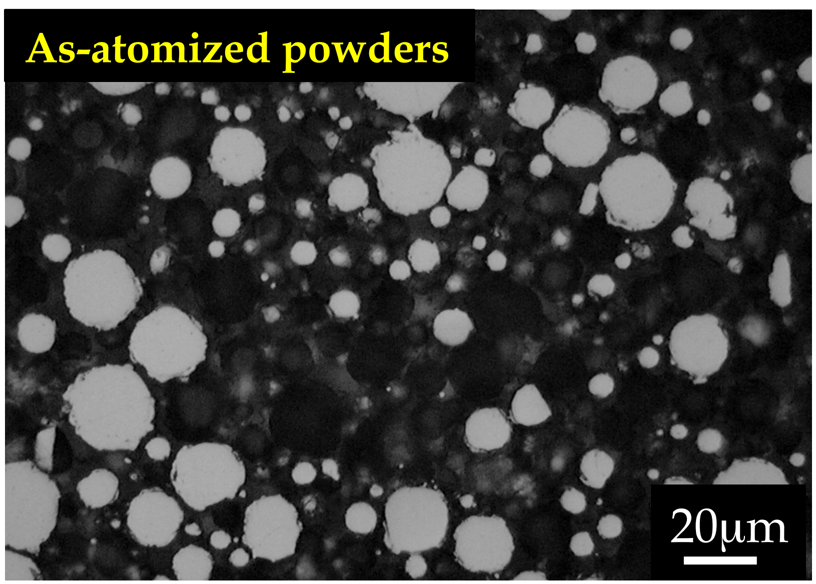

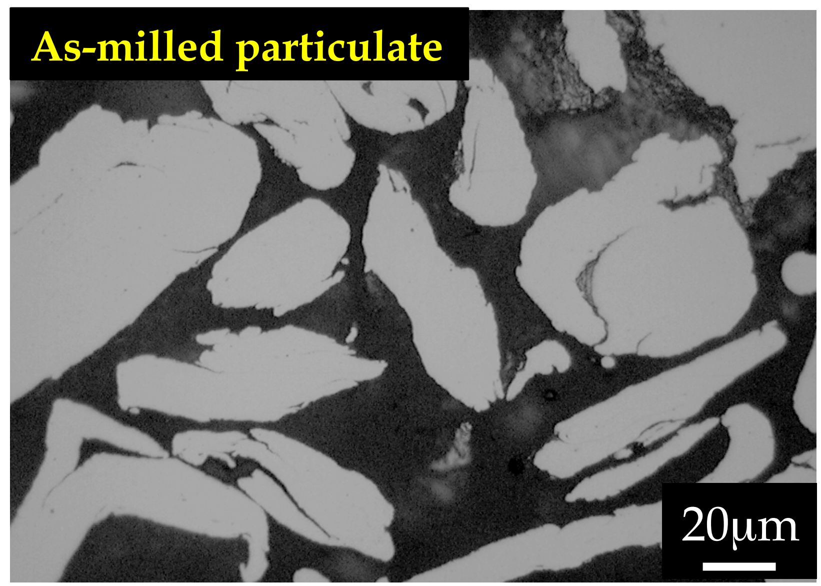

Alloy Design (Al Additions)

Fe-15.6Cr-10**Al**-0.36**Hf**-0.12Y at%
(Fe-15Cr-5**Al**-1.2**Hf**-0.2Y wt%)

Chill Cast Fingers	Polished (6 mm cubes)	Cr/Cr_2O_3 Rhines Pack (controlled P_{O_2})	Heat treated at 1200°C
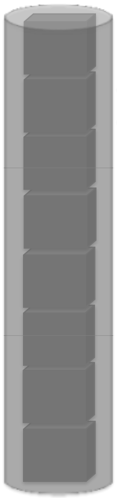	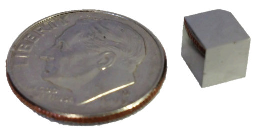		

- Simulate and identify internal O-exchange reactions within Fe-base alloys containing Al additions

- Evaluate the ability to form and sustain mixed Y-Hf-O dispersoids with Al present in the α-Fe matrix

- Resist YAG/YAM/YAP oxide dispersoid formation

- L. Zhang et al., Acta Mat. 57, 2009

Microstructure Evolution

Fe-15.6Cr-10**Al**-0.36**Hf**-0.12Y at%
(Fe-15Cr-5**Al**-1.2**Hf**-0.2Y wt%)

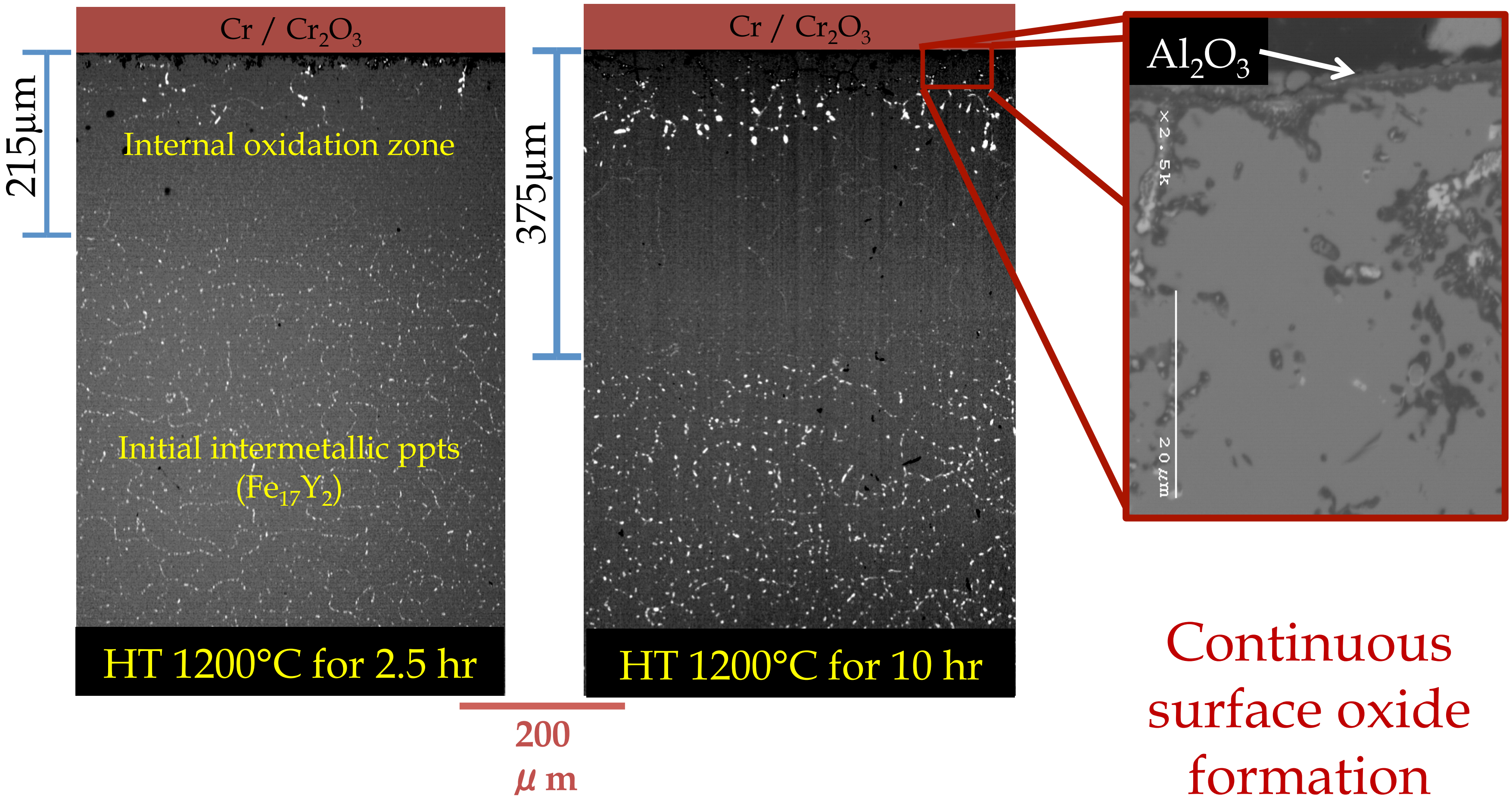

Continuous surface oxide formation

Preliminary Phase Analysis (serial XRD)

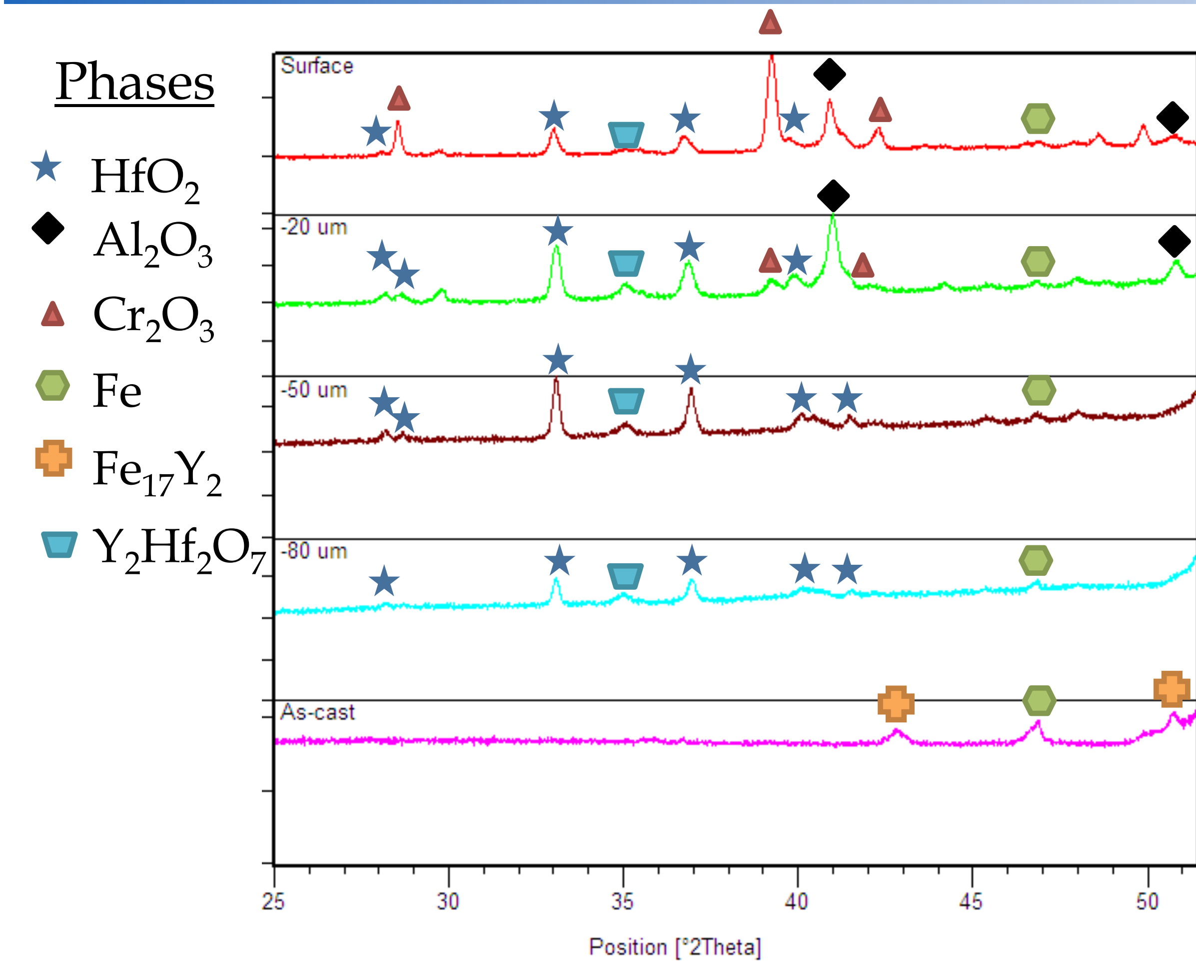

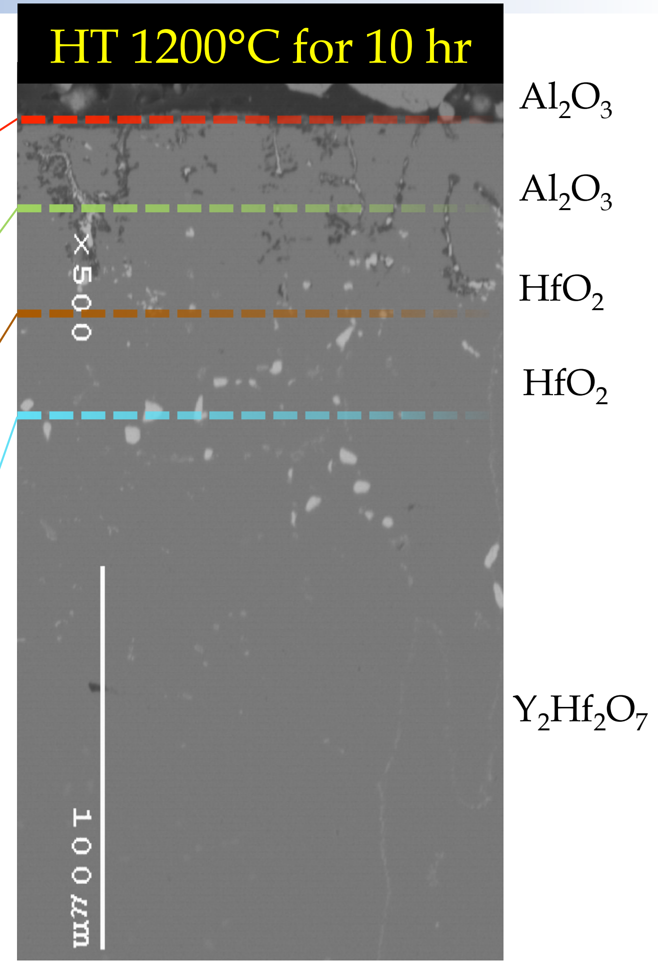

- Continuous surface layer of α-Al$_2$O$_3$
- No detectable Y$_3$Al$_5$O$_{12}$ (YAG), YAlO$_3$ (YAP), or Y$_4$Al$_2$O$_9$ (YAM) at the surface or within the internal oxidation zone
- **Mixed Y-Hf-O (Y$_2$Hf$_2$O$_7$) throughout the internal oxidation zone**

Conclusions

- GARS was successfully demonstrated as a simplified method to produce precursor powders for ODS ferritic stainless steel alloys
- Droplet cooling curves were used to formulate a theoretical oxidation model to accurately predict the resulting surface oxide layer thickness
- Microstructural results showed a clear ability to manipulate oxide and intermetallic phases within each CR-alloy using elevated temperature consolidation and heat treatment
- Phase analysis confirmed the operation of an O exchange reaction between PPB oxide and Y-enriched IMC precipitates, resulting in the formation of nano-metric dispersoids
- Initial Y-enriched IMC precipitate spatial distribution was shown to be highly dependent on powder particle size (i.e., solidification rate)

Conclusions

- Dispersoid thermal stability was enhanced through the addition of Hf as a substitute for Ti in these CR-alloys

- ODS microstructures fabricated from ultra-fine (dia. < 5μm) powders resulted in the most ideal spatial distribution of nano-metric oxide dispersoids (dia. < 10 nm)

- This solidification dependence suggests the need to modify the atomization processing parameters to dramatically increase the yield of ultra-fine powders, in order to achieve a more ideal ODS microstructure while maintaining this simplified processing scheme

- Initial elevated temperature mechanical testing revealed that these simplified CR-alloys contained a Y.S. similar to MA-956, while maintaining a threefold increase in total ductility

Acknowledgement

- This study was sponsored by the Department of Energy, Office of Fossil Energy (ARM program) through Ames Laboratory contract no. DE-AC02-07CH11358. The continued support of Bob Romanosky, Pat Rawls, Vito Cedro, and Richard Dunst is gratefully acknowledged.

- **Thanks to the Materials Preparation Center at Ames Laboratory, a U.S. Department of Energy Laboratory, for providing the processing tools and expertise to make this study possible (Larry Jones, Lanny Lincoln, Arne Swanson, Hal Sailsbury, Ross Anderson, David Boeke, and Trevor Riedemann).**

Disclaimer